ORIGINAL RESEARCH

Critical Role of Coaptive Strain in Aortic Valve Leaflet Homeostasis: Use of a Novel Flow Culture Bioreactor to Explore Heart Valve Mechanobiology

Katsuhide Maeda, MD, PhD; Xiaoyuan Ma, MD; Frank L. Hanley, MD; R. Kirk Riemer, PhD

***Background*—**Aortic valve (AV) disease presents critical situations requiring surgery in over 2% of the US population and is increasingly the reason for cardiac surgery. Throughout the AV cycle, mechanical forces of multiple types and varying intensities are exerted on valve leaflets. The mechanisms whereby forces regulate leaflet homeostasis are incompletely understood. We used a novel flow bioreactor culture to investigate alteration of AV opening or closure on leaflet genes.

***Methods and Results*—**Culture of rat AV was conducted in a flow bioreactor for 7 days at 37°C under conditions approximating the normal stroke volume. Three force condition groups were compared: Cycling (n=8); always open (Open; n=3); or always closed (Closed; n=5). From each culture, AV leaflets were pooled by force condition and RNA expression evaluated using microarrays. Hierarchical clustering of 16 transcriptome data sets from the 3 groups revealed only 2 patterns of gene expression: Cycling and Closed groups clustered together, whereas Open AV were different ($P<0.05$). Sustained AV opening induced marked changes in expression (202 transcripts >2-fold; $P<0.05$), whereas Closed AV exhibited similar expression pattern as Cycling (no transcripts >2-fold; $P<0.05$). Comparison with human sclerotic and calcific AV transcriptomes demonstrated high concordance of >40 Open group genes with progression toward disease.

***Conclusions*—**Failure of AV to close initiates an extensive response characterized by expression changes common to progression to calcific aortic valve disease. AV coaptation, whether phasic or chronic, preserved phenotypic gene expression. These results demonstrate, for the first time, that coaptation of valve leaflets is a fundamentally important biomechanical cue driving homeostasis. **(*J Am Heart Assoc*. 2016;5:e003506 doi: 10.1161/JAHA.116.003506)**

Key Words: animal model of human disease • gene expression/regulation • mechanical stretch • valve dynamics

The aortic valve (AV) transiently seals the outflow tract, a function critical to life. In the United States, valve diseases presenting situations requiring surgery account for nearly 20% of all cardiac surgeries.[1,2] Understanding of the mechanisms of homeostasis or deterioration of AV leaflet is critically important for management of valve disease in the clinical setting. Undergoing more than 40 million cycles per human year without wearing out, heart valves are normally quite durable tissues. This indicates a highly robust ability to self-repair, yet the mechanistic basis of this homeostatic maintenance and repair process is still poorly understood.

The question we pursued in this study is how the mechanical forces experienced by cycling AV affect normal leaflet homeostasis as well as the responses to its disruption by disease or mechanical intervention. To provide greater insight into the mechanisms actively mediating leaflet tissue homeostasis, we specifically asked how disruption of the valve cycle affected the normal expression program of AV leaflet genes. We developed a novel ex vivo AV flow-culture system with which we could systematically alter the forces to which leaflets are exposed in a controlled manner, and then study how disrupting cyclic valve coaptation modified leaflet gene expression.

In clinical settings, where valve closure is disrupted by aortic valve regurgitation, leaflets undergo negative remodeling of their extracellular matrix to a thickened and fibrotic state of reduced flexibility and elasticity.[3,4] This tissue-level

From the Pediatric Cardiac Surgery Division, Department of Cardiothoracic Surgery, Stanford University School of Medicine, Falk Cardiovascular Research Center, Stanford, CA.

Accompanying Tables S1 through S4 and Video S1 are available at http://jaha.ahajournals.org/content/5/7/e003506.full#sec-23

Presented at the 2015 American Heart Association Scientific Sessions; November 7–11, 2015; Orlando, FL.

Correspondence to: R. Kirk Riemer, PhD, Pediatric Cardiac Surgery Division, Department of Cardiothoracic Surgery, Falk Cardiovascular Research Center, Stanford University School of Medicine, 300 Pasteur Dr, Stanford, CA 94305-5407. E-mail: riemerk@stanford.edu

Received April 17, 2016; accepted June 27, 2016.

© 2016 The Authors. Published on behalf of the American Heart Association, Inc., by Wiley Blackwell. This is an open access article under the terms of the Creative Commons Attribution-NonCommercial License, which permits use, distribution and reproduction in any medium, provided the original work is properly cited and is not used for commercial purposes.

response to impaired coaptive stretch and disrupted flow conditions indicates a major role of blood-flow–induced mechanical forces (stretch, flow shear) in the maintenance of valve leaflet architecture.

In this report, we describe the effects of interrupting the AV cycle on leaflet gene expression. We found that alteration of the forces acting on AV by keeping valves open markedly increases the expression of multiple types of genes, whereas allowing them to undergo the coaptive stretch of closure and remain closed has essentially the same effect as allowing them to cycle.

Methods

Animals

Female Sprague-Dawley rats (250 g; Charles River Laboratories, Hollister, CA) were used for these studies under a Stanford University institutional review board–approved protocol. Under aseptic conditions, aortic valve grafts comprised of minimal myocardial cuff and aorta were harvested and mounted on sterile custom-fabricated cannula and stent fittings for anterograde flow. Both coronary arteries were ligated proximally to enable cyclic valve closure.

Novel Valve Culture Bioreactor System

We designed a novel bioreactor system specifically for use in these studies to replicate the normal valve cycle sequence: opening, closing, and pressurization by the arterial filling volume. It consisted of four main components: 500-mL medium reservoir (Corning, Edison, NJ); peristaltic roller pump (Masterflex; Cole-Parmer, Vernon Hills, IL); a custom-fabricated glass chamber serving as the ventricular surrogate; and a custom-fabricated acrylic afterload compliance chamber (Figure 1). Medium (EGM-2 MV; Lonza, Walkersville, MD) was continuously pumped in a pulsatile manner (Easy-load II pump head; Cole-Parmer) from the reservoir into the ventricular chamber in which 8 rat valve grafts underwent anterograde flow through individual outflow channels connected to a compliance chamber that provided an afterload filling volume for cyclic valve closure ("Cycling" condition) at 80 beats per minute (bpm) and returned medium to the reservoir. A separate outflow connection from the "ventricular" chamber shunted excess flow directly to the reservoir. Two force-designated groups of 4 valves each were studied—either Cycling and Open, or Cycling and Closed conditions—within a single culture experiment, keeping all other variables common. The rate of fluid flow through each Cycling valve graft was adjusted to achieve a complete valve cycle function at a moderate cycle rate (80 bpm; compared with ≈350-bpm normal rat heart rate) under a flow rate that approximated the known right ventricular stroke volume (160 μL) of the rat heart[5,6] and a pressure cycle (5–28 mm Hg).

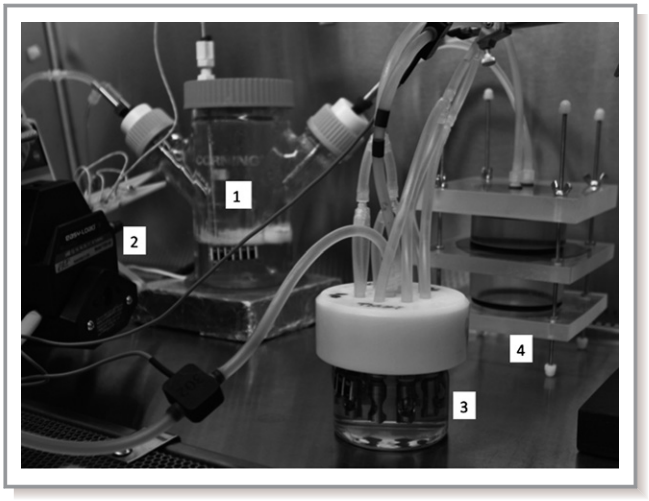

Figure 1. Bioreactor flow culture system for aortic valves. The principle components of the flow culture system are shown. Culture media in a 0.5-L volume glass side-arm flask reservoir (1) is heated to maintain 37°C with a surface heater. A peristaltic pump (2) moves media into a glass ventricular surrogate (3) reactor vessel (250-mL volume). A total of 8 intact rat aortic valves are mounted in a circular array inside the reactor (3) to provide physiologic anterograde flow. The outflows from the reactor vessel are connected to the afterload chamber (4). Outflow from the afterload chamber returns media to the reservoir (1).

Flow rate was monitored with inline ultrasonic flow probes (Transonic Systems Inc., Ithaca, NY). Bioreactor media was maintained at 37°C with a surface heater (Omega Engineering, Stamford, CT) beneath the reservoir and aerated with a gas mixture (5% CO_2, 21% O_2, and 74% N_2) to maintain a pH of 7.4.

Three different conditions of mechanical force were studied: Cycling, as described above, mimics normal physiological valve opening, closure, and full coaptation, indicating that the physiomimetic stretch loading of leaflets and pressurization of sinus by filling volume induces the normal transient coaptive stretch of leaflets. Second, an "Open" condition was used to sustain valve leaflets in a neutral-buoyancy, open state parallel to the outflow tract wall with minimal leaflet motion. The constantly open position state, in which AV experience neither stretch nor laminar flow shear, is a baseline zero point for forces acting on valves in which the only major force acting on the leaflets is the "ventricular" hydrostatic pressure. The third force condition we studied is that of the chronically closed valve (Closed) achieved by blocking forward flow distal to the valves. Full coaptation indicated physiomimetic stretch loading of leaflets.

Expression Microarray Analysis of Leaflet RNA

After 7 days of bioreactor culture, valve grafts were explanted to ice-cold PBS, then leaflets from each force condition group were harvested, pooled, and flash frozen in liquid nitrogen.

Total RNA was isolated from frozen leaflets with TRIzol reagent (Invitrogen, San Diego, CA) according to manufacturer's protocols, followed by an additional RNA purification with an RNAeasy Mini Kit (Qiagen, Redwood City, CA). Quality of RNA was assessed by UV absorption spectrophotometry (NanoDrop Technologies, ThermoFisher, Santa Clara, CA), and on-chip electrophoretic separation with quantitation (Bioanalyzer 2100; Agilent Technologies, Santa Clara, CA).

Intact total RNA from each sample pool was used for amplification, labeling, and hybridization on microarray slides for expression analysis. A total of 16 array data sets were thereby derived from 64 rats in 8 experiments using 8 aortic valves cultured under 2 force conditions in groups of 4 valves. Given that the Cycling condition is common to each experiment, there were 8 Cycling samples, 5 Closed, and 3 Open subjected to microarray analysis. Samples were hybridized on Rat Genome 230 2.0 Array slides (Affymetrix, Santa Clara, CA) using standard protocols for cRNA labeling, hybridization, and detection procedures. GeneSpring GX 12.6 (Agilent Technologies) software and the Partek Genomic Suite (version 6.6; St Louis, MO) were used for statistical analysis and to visualize the microarray data.

Statistical Analysis

The resulting raw array data CEL format files were uploaded to GeneSpring GX (version 12.6). Probe-level data were then compiled, normalized, and transformed using Robust Multichip Analysis. The following criteria were applied to filter the differentially expressed transcript list: a fold change of >2 and a Wilcoxon rank-sum test where $P<0.05$ with Benjamini-Hochberg estimation of false discovery rate (FDR). The resulting list of differentially expressed transcripts was uploaded into a BioBase ExPlain 3.1 data system (BIOBASE Biological database; Qiagen) and Ingenuity Pathway Analysis (IPA; Ingenuity Systems, Redwood City, CA) as the starting points for Gene Ontogeny (GO) analysis and generation of biological networks. In both systems, a *P* value is calculated to estimate the probability that each biological function and/or disease assigned to the data set of interest is not attributed to chance alone. Additionally, differentially expressed transcripts and genes are classified either by proprietary ontology's or by MESH terms according to the categories of canonical pathways, therapeutic target, biomarker, and molecular mechanism. The statistical significance of the association between the data set and the categories is estimated from the ratio of the number of proteins from the data set that map to the category divided by the total number of proteins that map to the canonical pathway. To define and identify patterns of gene expression profiles among the 3 valve culture groups (total n=16), unsupervised Hierarchical Clustering analysis was performed based on the values of the differentially expressed genes to determine the relatedness of expression patterns among the entire 16-sample group.

Real-time polymerase chain reaction (PCR) was performed as previously reported[7] to confirm expression of selected genes identified by microarray analysis. Briefly, total RNA from the 16 RNA pools used for array and additional experiments was reverse-transcribed (RT) to cDNA using the Superscript II RNase H Reverse Transcriptase kit (Invitrogen). An initial RT reaction minus RNA template confirmed that all RNA samples were free of contaminating genomic DNA. Forward and reverse gene-

Table 1. Primers Used for PCR Analysis

Gene	Primer for Human Gene	Amplicon Length (bp)	Gene Bank ID
Apln	TGCCTCCAGATGGGAAAGG CCCTGGTCCAGTCCTCGAA	80	AF179679
Aplnr	CCCTTCCTCTATGCCTTCTTTG TGGTCACAGCAGAGCATGGA	68	NM_031349
Cldn5	GCTGCCAGAGGAATGCGTTA GGGCAAGTCCTTTGGTTCAG	76	NM_031701
RT1-Da	CATCATCCAGGCGGAGTTCT CGTCACCGTCAAAGTCAAACA	71	NM_001008847
RT1-Ba	AGCCCCTGTGGAGGTCAAG CATATTTATACCATAGGCGGCTACGT	63	NM_001008831
RT1-Bb	AGAGTGTTTTGGTTGTGTTTGAAGAG GCAGGATTTGATGCGGAAA	67	NM_001004088
RT1-Db1	GACGCAGCCCCTGAAACA ACGCTGCCAGGGTAGAAGTC	66	NM_001008884
Pecam1	GGAAACCAACAGCCATTACGA AGGGAGGACACTTCCACTTCTG	69	NM_031591

bp indicates base pairs; PCR, polymerase chain reaction.

specific primers (Table 1) were used for quantitative real-time PCR analysis. Reactions were run on a ViiA 7 PCR instrument (Life Technologies, South San Francisco, CA), and mRNA levels were determined using the standard curve method. Expression values were normalized to the GAPDH expression level in a parallel reaction with the same amount of cDNA template. The fold change in expression was computed as the ratio of expression in Open condition divided by the expression in Cycling or Closed condition for paired tissue sample pools from each experiment in a total of 3 experiments per condition.

Results

AV Flow Culture Bioreactor System

The primary design strategy for the bioreactor system used in these studies (Figure 1) was to induce continuous cyclic opening and closing of the AV (Cycling condition) in a physiomimetic manner, which was verified visually and monitored by video during culture. Eight valves were cultured simultaneously (Figure 2A). Imaging under Cycling condition demonstrated complete closing (Figure 2B) and opening (Figure 2C) of valves with full coaptation of all leaflets, demonstrating valve competence. Our bioreactor system therefore replicates a normal valve functional cycle. A video recording of the valve dynamics during a typical culture experiment is provided in Video S1. In contrast to Cycling condition, we also cultured valves in a "Closed" condition to examine a state similar to the AV of nonpulsatile ventricular assist device (VAD) patients. The Closed condition induces full coaptation and thereby the physiomimetic stretch loading of leaflets that normally occurs transiently in Cycling valves, although considered a nonphysiological condition in general. A third, "Open" condition was also studied to model a state in which minimal forces are exerted on the AV, during which forward transvalvular flow was blocked distally and the leaflets remained in a constantly open position without laminar shear or strain forces. The Open condition was designed to create a high level of disruption of leaflet homeostasis and a baseline for the assessing effects of flow and coaptation on the self-maintenance process.

Force Alters Gene Expression in AV

Hierarchical clustering analysis of genes regulated in the Open group compared to the Cycling and Closed groups was performed to objectively assess the statistical heterogeneity in expression pattern among the 3 groups. The expression "heat" map array (Figure 3) depicts the hierarchical clustering dendrogram from this analysis. Two notable outcomes were apparent: First, based solely on their gene expression magnitude patterns, the 3 different culture conditions formed only 2 major clusters, the Open condition samples, and another cluster containing both Cycling and Closed condition samples. Second, expression changes observed in the Open group cluster were highly distinct from the other cluster, exhibiting a preponderance of upregulated genes (red bars in the heat map). Upregulation of gene expression in valves that stay open indicates that mechanical forces (laminar flow shear, stress, and strain) sustain a normally repressive effect on their expression. The clustering dendrogram at the top of Figure 3 shows that the Cycling and Closed groups are very highly related, even though the samples are from independent experiments in which the forces attendant to coaptation were experienced either phasic and cyclical or chronically static (Closed) for the culture duration.

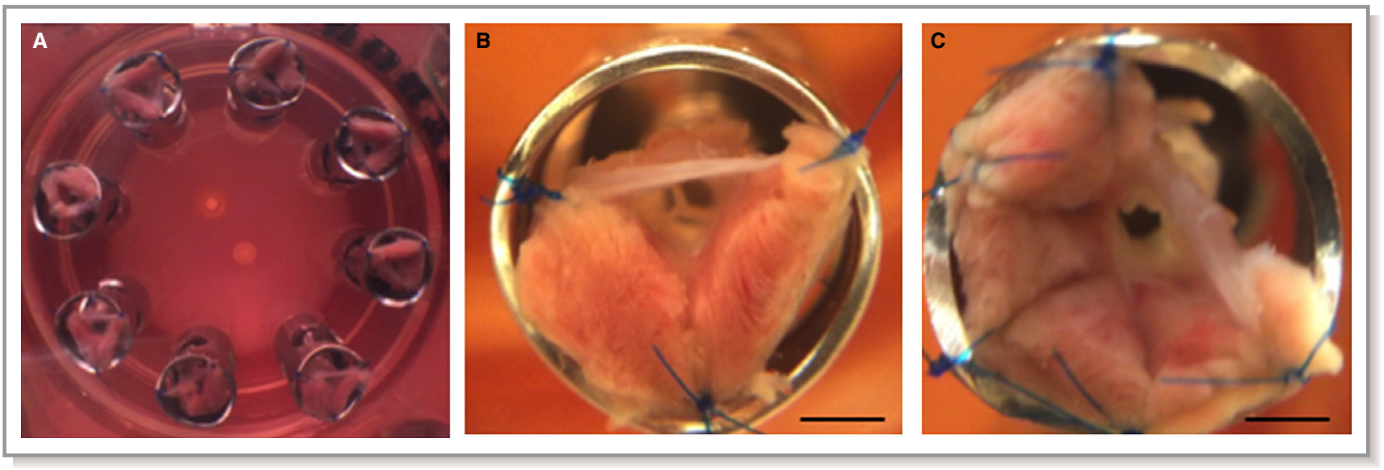

Figure 2. Flow-induced cyclic closure of rat aortic valves in flow culture. Eight valve grafts were cultured within the same experiment (A). Physiomimetic valve cycling was demonstrated by complete cyclic closing (B) and opening (C) of valves under flow condition. Ruler in (B and C), 5 mm. A video clip demonstrating cyclic closure is provided in Video S1.

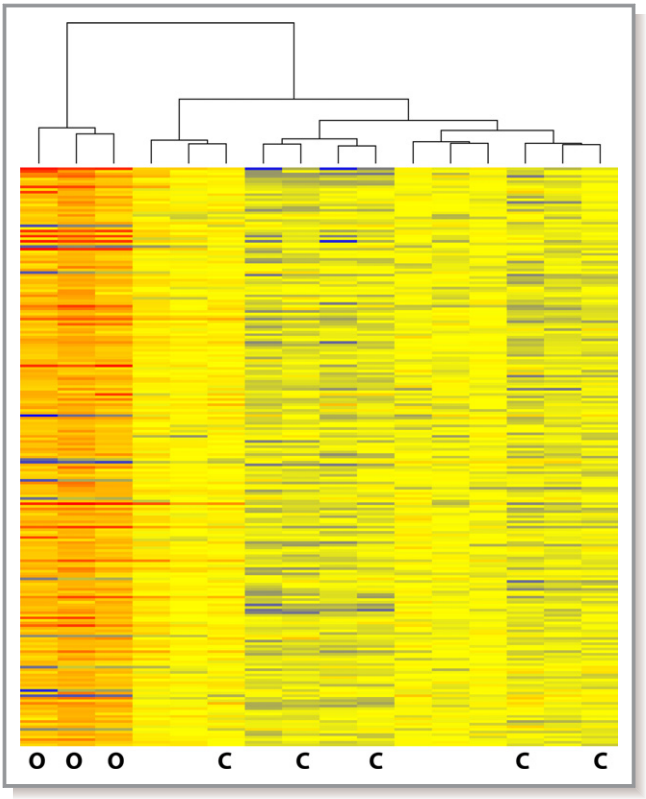

Figure 3. Hierarchical clustering analysis results arrayed as heat map. Transcriptome data for open, closed, and cycling AV were analyzed by hierarchical clustering and the results arrayed as heat map. The treatment condition is indicated below the data columns: O, Open (n=3); C, Closed (n=5), unlabeled, Cycling (n=8). The results of clustering analysis are represented by the dendrogram above the data columns. AV indicates aortic valve.

A summary of the up- and downregulated genes and their fold-change cutoff are listed in Figure 4A. We identified 202 genes in the Open valve group (fold >2.0; $P<0.05$, *t* test, followed by Benjamini and Hochberg FDR correction) that were differentially regulated compared with Cycling valves, and 211 genes in Open group versus Closed group comparison (Figure 4A). However, no significant differential expression was observed between the Cycling and Closed groups at the $P<0.05$ cutoff for >2-fold difference, indicating significant homogeneity of the 2 groups. Furthermore, the data of Figure 4A confirm the very high degree of overlap in expression values between Cycling and Closed valves. Table S1 lists the gene transcripts expressed >2-fold in the Open condition compared with the other 2 culture conditions. As shown in the Venn diagrams (Figure 4B and 4C), 190 differentially expressed transcripts were common between these 2 force condition groups (Figure 4B), and the majority of genes were upregulated. When Open valves were compared with either the Closed or Cycling valves, more than 90% of the >2-fold regulated transcripts were common to both groups. A similar high level of concordance was observed in the subsets of genes expressed at >4-fold (Figure 4A and 4C) and >10-fold changes. To further assess the homogeneity of the Closed and Cycling group transcriptomes, we compared the 28 transcripts regulated in the >1.2- to <2-fold change level and confirmed that the few differences between the 2 groups were of no apparent biological significance.

Genes Markedly Regulated in AV That Stay Open

In valves that stay open, we observed that over 30 genes were highly changed (>4-fold) in expression level. In Table 2, we list the top 10 upregulated and top 6 downregulated genes. The *P*-value scores for the significance of their fold change are also provided. The magnitude of change was far greater for upregulated genes, which comprised 4 genes classically associated with antigen presentation to immune cells and 3 genes for receptor molecules. The most downregulated genes code for molecules with diverse functions. Voltage-sensitive ion channel genes were also highly regulated: potassium channel (Kcne3) up- and chloride channel (Clcn4) downregulated.

Mechanical Force Regulates Multiple Gene Classes

We used GO analysis to classify the gene transcripts with altered expression between the Open and Cycling/Closed AV and quantitate their representation among 3 functional types: Molecular Function, Biological Process, and Cellular Components. Biological Process and Cellular Components were the predominantly represented classes at 45% and 40%, respectively. Molecular Function represented the smallest class at 15%.

Analysis using ExPlain 3.1 was used to explore statistically over-represented groups and identify significantly represented GO categories. In the regulated gene sets of both Open versus Cycling/Closed groups at a cutoff of $P<0.01$, over 120 GO classes were enriched. The most highly enriched GO classes include Cardiovascular System Development, Angiogenesis, and Cell Proliferation. Figure 5 shows the major GO listings of in these 2 analyses. Given the very high degree of overlap, we considered the Cycling and Closed groups as a single group and henceforth compared the Open and Cycling groups in the GO analysis reported below.

Functional Gene Pathway Analysis Identifies Key Canonical Pathways and Transcriptional Regulators

Functional analysis of genes with over 2-fold altered expression in the 3 different force conditions was conducted using IPA and several distinct relationships were identified. The

A

Fold Change	Open vs. Cycling		Open vs. Closed		Closed vs. Cycling	
	Up	Down	Up	Down	Up	Down
>2	190	12	200	11	0	0
>4	31	0	35	0	0	0
>10	8	0	8	0	0	0

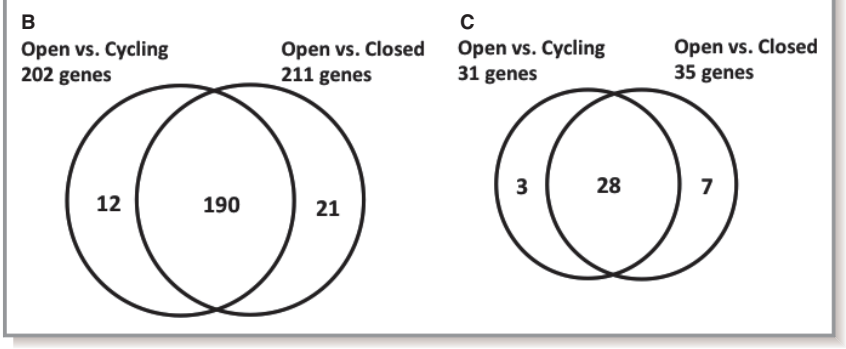

Figure 4. Integrated analysis of gene expression patterns. The data table (A) indicates the number of differentially regulated transcripts as a function of the fold-change cut-off value for the 3 comparison groups. Venn diagrams depict the transcripts with overlapping expression among the 3 culture conditions at a 2-fold change level (B) and a 4-fold change level (C) in the study group (1-way ANOVA corrected $P \leq 0.05$). The overlap in the Venn diagrams indicates the transcripts present in both comparisons.

major gene network functions identified were Cardiovascular system development and function, Organismal development, and Cardiovascular diseases. The statistically significant canonical pathways in each of the 3 different conditions are shown in Tables S2 and S3. Pathway activity analysis indicates the major canonical pathways that are activated

Table 2. List of the Top 10 Genes Up- and Down-regulated in Open Versus Cycling and Open Versus Closed Groups, Based on the Statistical Significance *P* Value

		Open vs Cycling		Open vs Closed	
Gene Symbol	Gene Annotation	Fold	*P* Value	Fold	*P* Value
Cd74	Cd74 molecule, major histocompatibility complex	17.64	2.09E-05	26.26	1.20E-05
Tifab	TRAF-interacting protein with forkhead-associated domain	17.57	4.13E-04	16.69	8.93E-04
RT1-Da	Major histocompatibility complex, class II, Da	16.17	3.30E-06	23.38	1.94E-06
RT1-Bb	Major histocompatibility complex, class II, Bb	15.51	1.90E-09	20.16	2.77E-08
RT1-Ba	Major histocompatibility complex, class II, Ba	13.60	3.33E-08	17.61	1.51E-09
Kcne3	Potassium voltage-gated channel, Isk-related family 3	12.73	1.02E-03	11.04	2.75E-03
RT1-Db1	Major histocompatibility complex, class II, Db1	10.79	1.31E-07	12.34	1.67E-07
Aplnr	Apelin receptor	10.69	2.67E-05	11.17	4.71E-05
Kdr	Kinase insert domain receptor	10.39	1.07E-03	11.86	1.26E-03
Cldn5	Claudin 5	9.15	7.58E-07	8.54	2.50E-06
Scrn1	Secernin 1	−2.41	2.16E-04	−2.52	2.70E-04
Clcn4	Chloride channel, voltage-sensitive 4	−2.30	1.15E-03	−2.42	2.59E-03
Pdlim3	PDZ and LIM domain 3	−2.74	3.10E-05	−2.68	8.16E-05
Slc6a15	Solute carrier family 6, member 15	−3.34	8.29E-04	−3.59	9.56E-04
Scx	Scleraxis	−3.66	1.37E-05	−2.77	2.74E-04
Mlana	Melan-A	−3.89	7.91E-05	−3.50	3.30E-04

P value adjusted by Benjamini and Hochberg false discovery rate correction.

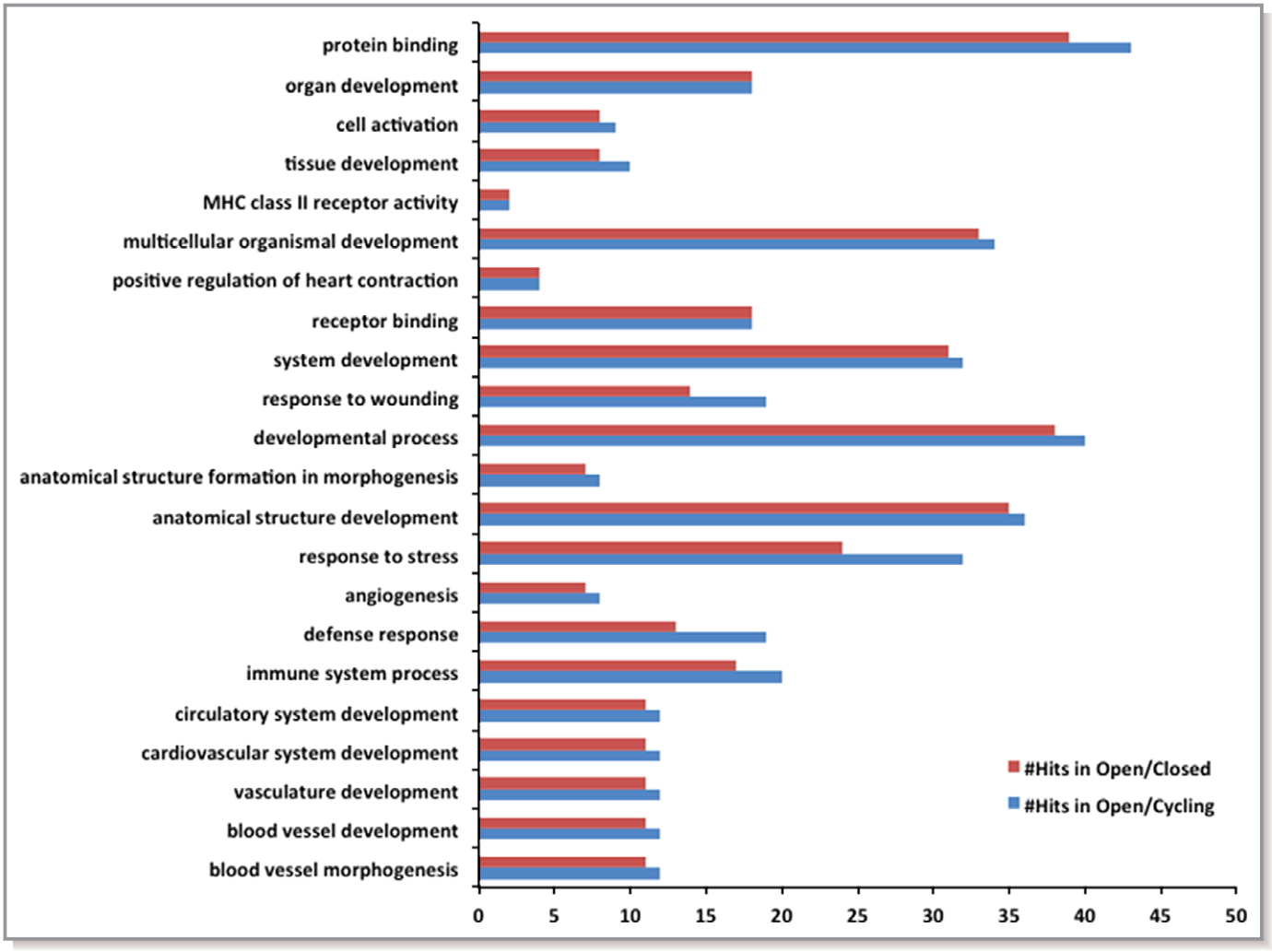

Figure 5. Gene ontology in open valve upregulated genes. Enriched Gene Ontology (GO) categories are identified along with number of genes in each category. Blue bars represent actual enriched number of genes in Open versus Cycling AV, whereas red bars represent actual enriched number of genes in Open versus Closed AV. The *x*-axis indicates the number of genes in each category ("Hits"). AV indicates aortic valve; MHC, major histocompatibility complex.

with *z*-score >2.0. IPA upstream regulator analysis identified 58 activated and 17 inhibited regulators in Open versus Cycling. The top regulator genes are vascular endothelial growth factor (VEGF), fibroblast growth factor 2 (FGF2), tumor necrosis factor (TNF), hypoxia-inducible factor (HIF) 1alpha, and nuclear factor kappa B (NF-κB) complex (Table 3). In Table 4, we compare the genes common to the 5 most represented pathways. The detailed list of the genes targeted by these 5 regulator genes is provided in Table S4.

Force-Regulated Rat AV Genes Are Also Active in Progression of Human AV Disease

We compared the transcripts regulated in Open AV with published transcriptome data for human diseased AV. The National Center for Biotechnology Information Gene Expression Omnibus (GEO) Datasets collection was used to access transcriptome data (GSE51472) for 3 groups in a total of 15 leaflet specimens of human AV: presclerotic (normal),

Table 3. Listing of Top Upstream Analysis-Predicted Activation State in Differentially Regulated Genes

Upstream Regulator	Molecule Type	Predicted State	Activation *z*-Score	*P* Value of Overlap
TNF	Cytokine	Activated	3.327	4.84E-11
VEGF	Group	Activated	3.516	4.21E-09
HIF1A	Transcription regulator	Activated	2.657	6.87E-09
FGF2	Growth factor	Activated	3.50	1.87E-07
NF-κB	Complex	Activated	3.227	3.01E-06

FGF2 indicates fibroblast growth factor 2; HIF1A, hypoxia-inducible factor 1A; NF-κB, nuclear factor kappa B; TNF, tumor necrosis factor; VEGF, vascular endothelial growth factor.

Table 4. Common Target Genes Activated in the Top Upstream Regulators

TNF Regulator	Vegf Regulator	HIF1A Regulator	FGF2 Regulator	NF-κB Regulator	Fold Change
ADORA2A	ADORA2A				2.06
ANGPT2	ANGPT2		ANGPT2		5.33
APLN	APLN	APLN			3.48
BDNF		BDNF	BDNF	BDNF	2.42
CCR5		CCR5			2.52
CXCR4	CXCR4	CXCR4	CXCR4	CXCR4	2.22
	DLL4	DLL4	DLL4		2.13
EFNA1	EFNA1			EFNA1	2.16
IGFBP3	IGFBP3	IGFBP3	IGFBP3		4.03
IL1B		IL1B	IL1B	IL1B	2.11
KDR	KDR		KDR	KDR	10.39
LYVE1	LYVE1		LYVE1		3.37
Notch4	Notch4		Notch4		2.63
NR5A2	NR5A2				2.07
PECAM1	PECAM1			PECAM1	2.16
PLK2				PLK2	2.67
SLC2A1		SLC2A1	SLC2A1	SLC2A1	2.24
VEGFA	VEGFA	VEGFA	VEGFA	VEGFA	2.69

FGF2 indicates fibroblast growth factor 2; HIF1A, hypoxia-inducible factor 1A; NF-κB, nuclear factor kappa B; TNF, tumor necrosis factor; VEGF, vascular endothelial growth factor.

sclerotic, and calcific AV generated by Ohukainen et al.[8] and available at GEO (http://www.ncbi.nlm.nih.gov/gds/?term=GSE51472). Multiple genes that we identified as significantly upregulated in Open rat AV are also reported to be upregulated progressively with advancing human AV disease (Table 5). Overall, more than 40 genes identified as upregulated in Open rat AV are also upregulated in Human AV exhibiting precalcific sclerosis and in calcific AV disease. For example, CXCR4, CD74, ADAMTS9, HLA-DA1, ANGPT2, and KDR were upregulated in both human and rat AV cultured under Open condition.

PCR Validation of Differentially Expressed Genes

To confirm the differential expression observed in microarray analyses, we performed quantitative real-time RT-PCR analysis (Table 6) of 8 representative genes: Apelin (Apln); apelin receptor (Aplnr); claudin5 (Cldn5); endothelial cell adhesion molecule 1 (Pecam1); and a group of the highest regulated gene family: Rattus norvegicus RT1 class II antigen (Ba, Bb, Da, and Db1), orthologs of human MHC classes II B and D. Upregulation in Open condition was confirmed in all 8 genes. For these confirmed genes, RT-PCR results represent a 90% concordance with the microarray data (ie, highest expression level of those genes with high signal intensity on the microarray).

Discussion

Heart valves continuously undergo changes in mechanical forces. The cyclical patterns of force change are sensed by valve leaflet endothelial and interstitial cells (VEC and VIC), and encoded as homeostatic signals that are still poorly understood. The focus of this study is the role of coaptive stretch forces on AV leaflet phenotype. We used a novel flow culture bioreactor system to isolate the separate effects of stretch and flow on rat AV grafts cultured either with normal cycling and forward flow, or without cycling or flow and constantly open (Open condition). In addition, we studied leaflet coaptive stretch in isolation by culturing with the AV constantly closed (Closed condition). The primary question we posed is how these 3 force conditions differentially affected leaflet gene expression patterns. We found that in valves remaining open during culture, multiple genes are expressed at much higher levels than in valves that close, whether closure is tonic or cyclic. This result demonstrated that valves that stay open (with leaflets unstretched) undergo activation of multiple gene expression pathways associated with valve remodeling or repair.

Analysis of our microarray expression data demonstrated that 2 signaling pathways were prominently activated when coaptive stretch was prevented: angiogenesis and Hif1alpha-directed hypoxia (Hif) signaling. The increased expression of angiogenic genes is consistent with a response to repair

Table 5. Regulated Rat AV Genes also Expressed in Human Diseased AV

Rat AV This Study			Human AV
Genes	Fold	Description	Gene
Acp5	5.04	Acid phosphatase 5, tartrate resistant	ACP5
Adamts9	3.20	ADAM metallopeptidase with thrombospondin type 1 motif	ADAMTS9
Angpt2	5.33	Angiopoietin 2	ANGPT2
Ccr5	2.52	Chemokine (C-C motif) receptor 5	CCR5
Cd74	17.64	Cd74 molecule, major histocompatibility complex, class II	CD74
Chst1	2.85	Carbohydrate (keratan sulfate Gal-6) sulfotransferase 1	CHST1
Cldn5	9.15	Claudin 5	CLDN5
CXCR4	2.22	Chemokine (C-X-C motif) receptor 4	CXCR4
RT1-Ba	13.60	Major histocompatibility complex, class II	HLA-DQA1
RT1-Bb	15.51	Major histocompatibility complex, class II	HLA-DQB1
RT1-Da	16.17	Major histocompatibility complex, class II	HLA-DRA
RT1-Db	10.79	Major histocompatibility complex, class II	HLA-DRB1
Igfbp3	4.03	Insulin-like growth factor binding protein 3	IGFBP3
Kcne3	12.73	Potassium voltage-gated channel, Isk-related family 3	KCNE3
Kdr	10.39	Kinase insert domain receptor	KDR
Lyve1	3.37	Lymphatic vessel endothelial hyaluronan receptor 1	LYVE1
Pdk1	2.24	Pyruvate dehydrogenase kinase, isozyme 1	PDK1
Ptp4a3	2.15	Protein tyrosine phosphatase type IVA, member 3	PTP4A3
Stc1	2.44	Stanniocalcin 1	STC1
Tgm2	3.29	Transglutaminase 2, C polypeptide	TGM2

AV indicates aortic valve.

endothelial cell damage through proliferative replacement. VECs are believed to be the primary source of new VICs as well, through the process of endothelial to mesenchymal transdifferentiation that generates valve leaflet precursor cushion structures during valve development.[9] Activation of the Hif signaling pathway in Open valves raises the possibility that in the absence of coaptive stretch (and forward flow), these leaflets become oxygen deficient. Given that Hif activation was much less in Closed or Cycling valves, our data indicate that it is the chronic open, unstretched state, rather than an ambient nutrient deficiency, that drives Hif expression.

Table 6. Comparison of PCR and Microarray Expression Values

		Open vs Cycling		Closed vs Cycling		
Column ID	Gene	PCR	Array	PCR	Array	Gene Bank ID
1389651_at	Apln	3.68±1.86	3.48	1.56±0.70	1.23	AF179679
1379772_at	Aplnr	5.80±4.74	10.69	4.47±1.00	−1.04	NM_031349
1374104_at	Cldn5	9.19±2.57	9.15	2.32±1.89	1.07	NM_031701
1371514_at	CD31	ND	2.16	1.25±0.15	−1.07	NM_031591
1370883_at	RT1-Da	14.38±10.71	16.17	1.77±0.80	−1.45	NM_001008847
1377334_at	RT1-Ba	9.12±11.18	13.60	1.48±0.71	−1.29	NM_001008831
1371065_at	RT1-Bb	ND	15.51	2.10±1.16	−1.30	NM_001004088
1370383_a	RT1-Db1	12.52±2.36	10.79	1.62±0.63	−1.14	NM_001008884

Values are mean±SD of fold change in expression for n=3 independent determinations. ND indicates not determined; PCR, polymerase chain reaction.

The Hif pathway is also known to regulate angiogenesis, for example, in tumor growth and also drives fibrosis by Vegf, Angpt2, and Igf. Therefore, given that the 2 most highly targeted pathways identified in Open valves are also highly interactive, Hif may be the primary transcriptional regulator. It is conceivable that the absence of leaflet stretch impairs the delivery of oxygen as well as nutrients to the core of leaflets. It has been shown that leaflets exist on the verge of core hypoxia because of their lack of vascularization,[10] and that leaflet motion including coaptation helps to convectively deliver nutrients to the deeper regions of valves.[11,12] Indeed, human valves are in the 300- to 700-μm thickness range,[13] beyond the theoretical passive oxygen diffusion range of 100 μm[14] when unloaded, yet remain fully viable. Of note, AV area increases at least 20% to 30% at coaptation.[15] We speculate that this increase in leaflet area attributed to stretching may be accompanied by a sufficient reduction in leaflet thickness to significantly reduce the diffusion distance for oxygen. Consistent with an effect of stretch to facilitate leaflet oxygen delivery, we note that Closed AVs have the same low level of hypoxia-regulated gene expression as do Cycling valves, suggesting that sustained physiological stretch of closure may be sufficient to reduce the diffusion barrier for oxygen, even without the convective assistance of leaflet cycling between stretched and relaxed states.

The findings of this study identify coaptive leaflet strain as a driver of leaflet homeostatic maintenance: Closed and Cycling AVs have a similar level of gene expression, whereas Open AVs uniquely exhibit marked upregulation of genes common to all 3 groups. Surprisingly, a role of forward flow-mediated laminar shear force in homeostatic maintenance is not demonstrated by our results, given that forward flow was essentially absent from both Open and Closed conditions, yet gene expression was markedly different between these 2 conditions. The role of forward flow in regulating this gene expression response was further demonstrated to be minimal, given that closed valves that had no forward flow (Closed) had the same expression pattern as cycling valves with forward flow (Cycling). Therefore, although shear stress from forward flow and stretch from coaptation are expectedly interactive during normal valve cycling, our results indicate that flow has less influence on gene expression than does stretch. Importantly, flow shear is sensed by valve endothelium, which then indirectly regulates neighboring cells, whereas stretch is sensed directly by leaflet cells. The response of a larger cell population (VEC plus VIC) to direct stimulation by stretch, pressure, and torsion may partially explain the observed predominant effect of stretch on gene expression. Much of the literature on heart valve mechanobiology focuses on the role of laminar flow shear as a dominant driver of valve homeostasis.[3,11] This well-accepted role of flow is a conceptual extension from vascular endothelial cells (ECs) to VEC: Flow shear forces affect the biology of both VEC and vascular ECs with many similarities and some differences.[16–18] However, other forces acting on leaflets also clearly influence valve cellular biology.[19] Elevated transvalvular pressure (eg, in the setting of hypertension) is a recognized risk factor for commissural fusion during VAD therapy as well as valvular diseases presumably attributed to the increased static pressure on valve cells and the increased strain loading on the closed AV root.[13,20] Connelly et al Leaflet stretch is recognized as an integral part of the valve cycle in studies of valve mechanics,[19] though apparently considered a force the leaflet must endure to prevent pathology rather than a driver of valve homeostasis. Importantly, in the conditions of our study, chronically Closed valves had no laminar shear flow exposure, and were chronically stretched, demonstrating that chronic closure was not a strong inducer of altered transcription compared with AV that stay open and unstretched. Our results therefore provide strong evidence that the physiological straining of leaflets may be a major regulator of leaflet homeostasis. Expanded analysis of the AV tissue in our study and of the biological roles of the differentially expressed genes will help to confirm these intriguing initial findings.

Many of the genes regulated in Open AV are also regulated in human sclerotic and calcific valves based upon a comparison of published transcriptome data sets.[8] Overall, more than 40 genes identified as upregulated in Open condition rat AV are also reported to be upregulated in human AV exhibiting precalcific sclerosis and in calcific AV disease (Table 5). This congruence in disease-related gene expression changes across species demonstrates the potential clinical relevance of our ex vivo AV culture system as a platform for exploring the mechanisms through which mechanical forces regulate leaflet homeostasis. Furthermore, our study results therefore support the concept that reduced leaflet tissue nutrient and/or oxygen delivery may be a causative factor in human valve disease progression in a feed-forward manner as leaflets thicken because of disease, or even simply aging.

Limitations

Changes in mRNA are inferred as changes in the biology relevant to this study. Although alterations in gene expression indicate definite cell-level responses typically orchestrated at the nuclear level, they do not necessarily inform about potentially important changes at the levels of stored-protein release, protein catalytic activity, and post-translational modifications, such as phosphorylation and other subcellular signaling, which must be directly measured. RNA

changes are informative, but we acknowledge that they are just a starting point to understanding how systems are modified by the perturbations under study. The observed changes necessarily constitute averages over the entire valve leaflets, so focal changes in a specific region and/or cell type may not be detected, and small changes may be obscured. Appreciating this reality, we have emphasized the most significant changes pending follow-up analyses in ongoing studies.

The conditions of heart rate and pressure gradients present in this ex vivo culture system are both significantly lower than normal or peak in vivo levels of rats (ca 400 bpm and 90 mm Hg). This was deliberate and necessitated by limitations of the bioreactor system, which does nonetheless replicate what our data demonstrate to be critically important aspects of valve physiology. We note that preserving flow rate and valve sinus pressurization was sufficient to reveal significant differences in gene expression that we demonstrate to be consistent with and parallel to human calcific aortic valve disease, demonstrating that model systems in other species need not fully replicate in vivo physiology in order to reveal important biological mechanisms relevant to human disease. Importantly, it has been demonstrated that a pressure of 20 mm Hg is sufficient to completely uncrimp (relax and extend) the collagen fibrils of the aortic valve leaflet.[21] Beyond this pressure, the AV leaflets resist stretch and act more like tendons. Because our focus was the role of leaflet stretch on homeostasis, the pressure range we studied is therefore more than adequate to achieve full stretch. Above 20 mm Hg to the peak systolic range of 90 mm Hg, compression of leaflets occurs and this force is expectedly sensed by all leaflet cells; an up to 30% further increase in VIC nuclear deformation is reported to occur between 20 and 90 mm Hg.[22] Therefore, though our studies likely capture the full effect of leaflet stretch, they do not fully capture in vivo–level compressive forces and this limitation is acknowledged. The design and implementation of a bioreactor system that replicates additional aspects rat physiology is underway for the further investigation of our results. The additional increment in peak pressure to 90 mm Hg could conceivably alter the magnitude of the changes we observed; whether different genes become regulated will be determined in future studies.

Summary and Conclusions

In summary, we used gene expression profiling to assess the effects of disrupting normal aortic valve cyclic closure in a flow culture bioreactor model system. Valves that stay open and remain without the strain of coaptation exhibit high-magnitude changes in the expression of many genes. Valves that remain closed with a physiological level of coaptive stretch exhibit a gene profile that essentially the same as that of cycling valves. Of note, comparing our results with published transcriptome data of human AV disease specimens revealed that many of the genes we observed as upregulated in rat AVs are also increased in human AVs exhibiting stenosis-induced sclerosis and also valves with calcific disease. We therefore conclude that disruption of the normal mechanical forces upon valves, coaptive strain in particular, is sufficient to markedly alter their gene expression in a manner similar to that associated with human valvular disease. Our results also demonstrate that the absence of laminar flow shear (Open and Closed AV) may be of less critical importance relative to coaptive stretch, and this is a surprising finding, the implication/relevance of which needs to be further explored to be better understood.

Sources of Funding

This work was supported by the Lucile Packard Foundation for Children's Health, Alex Vibber Endowment (to Hanley), and the Oak Foundation (Grant No.: OUSA-07-096; to Hanley).

Disclosures

None.

References

1. Nkomo VT, Gardin JM, Skelton TN, Gottdiener JS, Scott CG, Enriquez-Sarano M. Burden of valvular heart diseases: A population-based study. *Lancet*. 2006;368:1005–1011.
2. Iung B, Vahanian A. Epidemiology of valvular heart disease in the adult. *Nat Rev Cardiol*. 2011;8:162–172.
3. Gould ST, Srigunapalan S, Simmons CA, Anseth KS. Hemodynamic and cellular response feedback in calcific aortic valve disease. *Circ Res*. 2013;113:186–197.
4. Freeman RV, Otto CM. Spectrum of calcific aortic valve disease: pathogenesis, disease progression, and treatment strategies. *Circulation*. 2005;111:3316–3326.
5. Deten A, Millar H, Zimmer HG. Catheterization of pulmonary artery in rats with an ultraminiature catheter pressure transducer. *Am J Physiol Heart Circ Physiol*. 2003;285:H2212–H2217.
6. Faber MJ, Dalinghaus M, Lankhuizen IM, Steendijk P, Hop WC, Schoemaker RG, Duncker DJ, Lamers JM, Helbing WA. Right and left ventricular function after chronic pulmonary artery banding in rats assessed with biventricular pressure-volume loops. *Am J Physiol Heart Circ Physiol*. 2006;291:H1580–H1586.
7. Ma X, Barboza LA, Siyahian A, Reinhartz O, Maeda K, Reddy VM, Hanley FL, Riemer RK. Tetralogy of fallot: aorto-pulmonary collaterals and pulmonary arteries have distinctly different transcriptomes. *Pediatr Res*. 2014;76:341–346.
8. Ohukainen P, Syvaranta S, Napankangas J, Rajamaki K, Taskinen P, Peltonen T, Helske-Suihko S, Kovanen PT, Ruskoaho H, Rysa J. MicroRNA-125b and chemokine CCL4 expression are associated with calcific aortic valve disease. *Ann Med*. 2015;47:423–429.
9. Armstrong EJ, Bischoff J. Heart valve development: Endothelial cell signaling and differentiation. *Circ Res*. 2004;95:459–470.
10. Weind KL, Boughner DR, Rigutto L, Ellis CG. Oxygen diffusion and consumption of aortic valve cusps. *Am J Physiol Heart Circ Physiol*. 2001;281:H2604–H2611.
11. Back M, Gasser TC, Michel JB, Caligiuri G. Biomechanical factors in the biology of aortic wall and aortic valve diseases. *Cardiovasc Res*. 2013;99:232–241.

12. Wang L, Korossis S, Fisher J, Ingham E, Jin Z. Prediction of oxygen distribution in aortic valve leaflet considering diffusion and convection. *J Heart Valve Dis*. 2011;20:442–448.

13. May-Newman K, Mendoza A, Abulon DJK, Joshi M, Kunda A, Dembitsky W. Geometry and fusion of aortic valves from pulsatile flow ventricular assist device patients. *J Heart Valve Dis*. 2011;20:149–158.

14. Dasika SK, Kinsey ST, Locke BR. Reaction-diffusion constraints in living tissue: Effectiveness factors in skeletal muscle design. *Biotechnol Bioeng*. 2011; 108:104–115.

15. Balachandran K, Sucosky P, Yoganathan AP. Hemodynamics and mechanobiology of aortic valve inflammation and calcification. *Int J Inflam*. 2011;2011: 263870.

16. Butcher JT, Nerem RM. Valvular endothelial cells regulate the phenotype of interstitial cells in co-culture: Effects of steady shear stress. *Tissue Eng*. 2006;12:905–915.

17. Butcher JT, Nerem RM. Valvular endothelial cells and the mechanoregulation of valvular pathology. *Philos Trans R Soc Lond B Biol Sci*. 2007;362:1445–1457.

18. Butcher JT, Penrod AM, Garcia AJ, Nerem RM. Unique morphology and focal adhesion development of valvular endothelial cells in static and fluid flow environments. *Arterioscler Thromb Vasc Biol*. 2004;24:1429–1434.

19. Thayer P, Balachandran K, Rathan S, Yap CH, Arjunon S, Jo H, Yoganathan AP. The effects of combined cyclic stretch and pressure on the aortic valve interstitial cell phenotype. *Ann Biomed Eng*. 2011;39:1654–1667.

20. Connelly JH, Abrams J, Klima T, Vaughn WK, Frazier OH. Acquired commissural fusion of aortic valves in patients with left ventricular assist devices. *J Heart Lung Transplant*. 2003;22:1291–1295.

21. Sacks MS, Smith DB, Hiester ED. The aortic valve microstructure: Effects of transvalvular pressure. *J Biomed Mater Res*. 1998;41:131–141.

22. Huang HY, Liao J, Sacks MS. In-situ deformation of the aortic valve interstitial cell nucleus under diastolic loading. *J Biomech Eng*. 2007;129:880–889.

SUPPLEMENTAL MATERIAL

Table S1. List of Differentially Regulated Genes in One Culture Condition Compared With the Other Culture Condition (fold>2.0, P<0.05).
Values are the numeric ratio of their expression level (calculated as the fold change; negative values indicate downregulation).

Gene ID	Gene Symbol	Open vs Cycling	Open vs Closed	Closed vs Cycling	Gene Title
1367679_at	Cd74	17.64	26.27	-1.49	Cd74 molecule, major histocompatibility complex, class II
1378418_at	Tifab	17.57	16.69	1.05	TRAF-interacting protein with forkhead-associated domain, family member B
1370883_at	RT1-Da	16.17	23.39	-1.45	RT1 class II, locus Da
1371065_at	RT1-Bb	15.51	20.16	-1.30	similar to RT1 class II histocompatibility antigen, B-1 beta chain precursor (RT1.B-bet
1377334_at	RT1-Ba	13.60	17.61	-1.29	RT1 class II, locus Ba
1387160_at	Kcne3	12.73	11.04	1.15	potassium voltage-gated channel, Isk-related family, member 3
1370822_at	RT1-Ba	11.58	15.54	-1.34	RT1 class II, locus Ba
1370383_s_at	RT1-Db1	10.79	12.35	-1.14	RT1 class II, locus Db1
1379772_at	Aplnr	10.69	11.17	-1.04	apelin receptor
1367948_a_at	Kdr	10.39	11.86	-1.14	kinase insert domain receptor
1374104_at	Cldn5	9.15	8.54	1.07	claudin 5
1368294_at	Dnase1l3	8.15	9.25	-1.13	deoxyribonuclease 1-like 3
1374546_at	Pcdh17	7.76	8.40	-1.08	protocadherin 17
1383824_at	Ldb2	7.65	7.22	1.06	LIM domain binding 2
1384603_at	Abca4	7.47	7.07	1.06	ATP-binding cassette, subfamily A (ABC1), member 4
1384907_at	LOC306096	7.01	7.75	-1.11	similar to Dachshund homolog 1 (Dach1)
1393452_at	Car9	5.97	6.20	-1.04	carbonic anhydrase 9
1368052_at	Tspan8	5.90	7.11	-1.20	tetraspanin 8
1381771_at	---	5.59	5.61	-1.00	---

1374207_at	Angpt2	5.33	5.06	1.05	angiopoietin 2
1387050_s_at	Kng1	5.25	4.34	1.21	kininogen 1 /// kininogen 1-like 1 /// kininogen 2
1378569_at	---	5.15	5.92	-1.15	---
1367942_at	Acp5	5.04	5.52	-1.10	acid phosphatase 5, tartrate resistant
1374863_at	Rbp7	4.83	5.79	-1.20	retinol binding protein 7, cellular
1390849_at	---	4.77	4.59	1.04	---
1377626_at	LOC100911030	4.75	4.97	-1.05	uncharacterized LOC100911030
1373957_at	Reln	4.65	3.57	1.30	reelin
1379985_at	---	4.47	4.22	1.06	---
1393559_at	---	4.37	4.23	1.03	---
1388602_at	Cfd	4.26	3.69	1.15	complement factor D (adipsin)
1367930_at	Gap43	4.12	4.94	-1.20	growth associated protein 43
1381971_at	Sox18	4.04	4.62	-1.14	SRY (sex determining region Y)-box 18
1386881_at	Igfbp3	4.03	3.16	1.27	insulin-like growth factor binding protein 3
1393411_at	Cfp	4.02	3.73	1.08	complement factor properdin
1387154_at	LOC100912228 /// Npy	3.97	3.68	1.08	pro-neuropeptide Y-like /// neuropeptide Y
1384415_at	Sox7	3.85	4.60	-1.19	SRY (sex determining region Y)-box 7
1395859_at	---	3.85	3.70	1.04	---
1376624_at	---	3.84	4.59	-1.20	---
1397593_at	---	3.80	4.06	-1.07	---
1374491_at	Cmtm8	3.73	4.32	-1.16	CKLF-like MARVEL transmembrane domain containing 8
1368578_at	Hsd3b1	3.65	4.21	-1.15	hydroxy-delta-5-steroid dehydrogenase, 3 beta- and steroid delta-isomerase 1
1371883_at	Mmd	3.57	3.63	-1.02	monocyte to macrophage differentiation-associated
1393627_at	Mgarp	3.55	3.56	-1.00	mitochondria-localized glutamic acid-rich protein
1368723_at	Lat	3.55	3.54	1.00	linker for activation of T cells
1387273_at	Il1rl1	3.53	2.48	1.43	interleukin 1 receptor-like 1
1384262_at	Ppp1r3b	3.53	3.96	-1.12	protein phosphatase 1, regulatory subunit 3B
1382580_at	---	3.49	4.12	-1.18	---

1389651_at	Apln	3.48	2.83	1.23	apelin
1372761_at	---	3.48	4.06	-1.17	---
1369093_at	Reln	3.47	3.06	1.13	reelin
1393227_at	---	3.42	3.08	1.11	---
1373777_at	---	3.41	3.80	-1.11	---
1382732_at	Lyve1	3.37	3.06	1.10	lymphatic vessel endothelial hyaluronan receptor 1
1383935_at	---	3.37	3.44	-1.02	---
1372213_at	LOC500300	3.32	3.37	-1.01	similar to hypothetical protein MGC6835
1369943_at	Tgm2	3.29	3.48	-1.06	transglutaminase 2, C polypeptide
1380616_at	St8sia4	3.28	3.58	-1.09	ST8 alpha-N-acetyl-neuraminide alpha-2,8-sialyltransferase 4
1385682_at	Vit	3.28	2.98	1.10	vitrin
1379114_at	---	3.22	3.54	-1.10	---
1381804_at	Bcl6b	3.21	3.30	-1.03	B-cell CLL/lymphoma 6, member B
1382192_at	Lyve1	3.21	2.89	1.11	lymphatic vessel endothelial hyaluronan receptor 1
1376481_at	Adamts9	3.20	3.51	-1.10	ADAM metallopeptidase with thrombospondin type 1 motif, 9
1390221_at	Prdm1	3.17	3.07	1.03	PR domain containing 1, with ZNF domain
1377646_at	---	3.15	3.17	-1.01	---
1377786_at	---	3.08	3.33	-1.08	---
1391251_at	---	3.04	2.79	1.09	---
1389763_at	---	3.03	3.20	-1.05	---
1390318_at	---	3.02	3.27	-1.08	---
1367652_at	Igfbp3	3.02	2.39	1.26	insulin-like growth factor binding protein 3
1377190_at	Fam65b	3.02	2.43	1.24	family with sequence similarity 65, member B
1391808_at	Arrdc4	3.01	3.84	-1.28	arrestin domain containing 4
1378833_at	---	3.01	2.68	1.12	---
1373336_at	Gprc5b	3.01	2.88	1.04	G protein-coupled receptor, family C, group 5, member B
1396884_at	---	3.00	3.18	-1.06	---
1392706_at	---	2.93	2.89	1.01	---
1384192_at	Chst1	2.85	3.31	-1.16	carbohydrate (keratan sulfate Gal-6) sulfotransferase 1
1376775_at	Prr5l	2.84	2.99	-1.05	proline rich 5 like

1373979_at	---	2.81	3.04	-1.08	---
1378783_at	---	2.77	2.94	-1.06	---
1374266_at	---	2.76	3.27	-1.19	---
1384667_x_at	Galr2 /// LOC100910349	2.73	3.22	-1.18	galanin receptor 2 /// galanin receptor type 2-like
1387389_at	Ramp3	2.71	3.00	-1.11	receptor (G protein-coupled) activity modifying protein 3
1373807_at	Vegfa	2.69	2.35	1.14	vascular endothelial growth factor A
1373301_at	Ppp1r13b	2.68	2.98	-1.11	protein phosphatase 1, regulatory subunit 13B
1368106_at	Plk2	2.67	2.87	-1.08	polo-like kinase 2
1374626_at	Lrg1	2.66	2.70	-1.02	leucine-rich alpha-2-glycoprotein 1
1377862_at	---	2.65	3.13	-1.18	---
1387776_at	Tgm2	2.64	2.84	-1.07	transglutaminase 2, C polypeptide
1382017_at	---	2.64	3.01	-1.14	---
1389847_at	Notch4	2.63	2.74	-1.04	notch 4
1392032_at	Grap	2.62	2.52	1.04	GRB2-related adaptor protein
1383844_at	Arhgef15	2.61	2.77	-1.06	Rho guanine nucleotide exchange factor (GEF) 15
1389297_at	Ero1l	2.61	2.62	-1.00	ERO1-like (S. cerevisiae)
1391453_at	Ebi3	2.57	2.45	1.05	Epstein-Barr virus induced 3
1370211_at	Nrgn	2.57	2.67	-1.04	neurogranin
1376328_at	RGD1310819	2.57	2.90	-1.13	similar to putative protein (5S487)
1384239_at	Tbc1d8	2.56	2.50	1.03	TBC1 domain family, member 8
1390412_at	LOC100911874 /// Slc40a1	2.53	2.69	-1.06	solute carrier family 40 member 1-like /// solute carrier family 40 (iron-regulated tra
1389656_at	LOC679462	2.53	2.47	1.02	similar to Tetraspanin-15 (Tspan-15) (Transmembrane 4 superfamily member 15) (Tetraspan
1372485_at	Pcbd1	2.52	2.51	1.01	pterin-4 alpha-carbinolamine dehydratase/dimerization cofactor of hepatocyte nuclear fa
1369290_at	Ccr5	2.52	2.39	1.05	chemokine (C-C motif) receptor 5
1391481_at	---	2.49	2.00	1.24	---
1382868_at	Sema6a	2.48	2.84	-1.14	sema domain, transmembrane domain (TM), and cytoplasmic domain, (semaphorin) 6A

1382130_at	Pcdh19	2.47	2.57	-1.04	protocadherin 19
1368097_a_at	Rtn1	2.47	2.55	-1.03	reticulon 1
1376909_at	Rasl10a	2.47	2.59	-1.05	RAS-like, family 10, member A
1372097_at	---	2.45	2.33	1.05	---
1383983_at	---	2.45	2.78	-1.13	---
1385451_at	St8sia4	2.44	2.40	1.01	ST8 alpha-N-acetyl-neuraminide alpha-2,8-sialyltransferase 4
1396101_at	Stc1	2.44	2.25	1.08	stanniocalcin 1
1382138_at	LOC100912697 /// Nrarp	2.42	2.65	-1.09	notch-regulated ankyrin repeat-containing protein-like /// Notch-regulated ankyrin repe
1393883_at	---	2.42	3.10	-1.28	---
1385798_at	---	2.42	2.70	-1.11	---
1368677_at	Bdnf	2.42	2.17	1.12	brain-derived neurotrophic factor
1384301_at	---	2.42	2.67	-1.11	---
1385051_at	Gbp4 /// LOC100911495	2.40	2.47	-1.03	guanylate binding protein 4 /// guanylate-binding protein 4-like
1379093_at	---	2.40	2.82	-1.18	---
1370081_a_at	Vegfa	2.39	2.05	1.17	vascular endothelial growth factor A
1378005_at	Sema6a	2.39	2.62	-1.10	sema domain, transmembrane domain (TM), and cytoplasmic domain, (semaphorin) 6A
1378869_at	---	2.39	2.65	-1.11	---
1384946_at	Tlr1	2.39	2.20	1.08	toll-like receptor 1
1390302_at	---	2.38	2.51	-1.05	---
1383692_at	Prelid2	2.38	2.42	-1.02	PRELI domain containing 2
1381409_at	---	2.38	2.44	-1.02	---
1389214_at	Lama4	2.37	2.48	-1.05	laminin, alpha 4
1375230_at	---	2.37	2.05	1.16	---
1378261_at	---	2.35	2.37	-1.01	---
1384920_at	---	2.35	2.40	-1.02	---
1376830_at	Exoc3l1	2.34	2.50	-1.07	exocyst complex component 3-like 1
1391690_at	Gpr114	2.33	2.59	-1.11	G protein-coupled receptor 114

1380908_at	---	2.32	2.36	-1.02	---
1377286_at	Gimap4	2.32	2.31	1.00	GTPase, IMAP family member 4
1387130_at	LOC100911874 /// Slc40a1	2.32	2.58	-1.11	solute carrier family 40 member 1-like /// solute carrier family 40 (iron-regulated tra
1371824_at	Ak4	2.31	2.44	-1.05	adenylate kinase 4
1375277_at	LOC100912697 /// Nrarp	2.31	2.37	-1.03	notch-regulated ankyrin repeat-containing protein-like /// Notch-regulated ankyrin repe
1382535_at	---	2.31	2.23	1.04	---
1394295_at	Tmem255a	2.31	2.37	-1.03	transmembrane protein 255A
1386798_at	---	2.31	2.86	-1.24	---
1373724_at	Krt4	2.30	2.20	1.05	keratin 4
1389198_at	Sh2d3c	2.30	2.39	-1.04	SH2 domain containing 3C
1396378_at	---	2.30	2.47	-1.08	---
1377041_at	Mfng	2.29	2.33	-1.02	MFNG O-fucosylpeptide 3-beta-N-acetylglucosaminyltransferase
1395141_at	---	2.29	2.31	-1.01	---
1390161_at	Cyyr1	2.29	2.48	-1.08	cysteine/tyrosine-rich 1
1373483_at	Kank3	2.28	2.44	-1.07	KN motif and ankyrin repeat domains 3
1378006_at	---	2.27	1.96	1.16	---
1381576_at	Pik3c2b	2.26	2.53	-1.12	phosphatidylinositol-4-phosphate 3-kinase, catalytic subunit type 2 beta
1371671_at	---	2.25	2.26	-1.01	---
1368079_at	Pdk1	2.24	2.19	1.03	pyruvate dehydrogenase kinase, isozyme 1
1373685_at	Ankrd37	2.24	2.32	-1.03	ankyrin repeat domain 37
1373818_at	---	2.24	2.01	1.11	---
1370848_at	Slc2a1	2.24	2.15	1.04	solute carrier family 2 (facilitated glucose transporter), member 1
1389285_at	Mpp3	2.24	2.45	-1.10	membrane protein, palmitoylated 3 (MAGUK p55 subfamily member 3)
1391856_at	Sema3g	2.23	2.31	-1.04	sema domain, immunoglobulin domain (Ig), short basic domain, secreted, (semaphorin) 3G
1370905_at	Dock9	2.23	2.34	-1.05	dedicator of cytokinesis 9
1370097_a_at	Cxcr4	2.22	1.97	1.13	chemokine (C-X-C motif) receptor 4
1384626_at	---	2.19	2.02	1.09	---
1389353_at	Sema6d	2.18	2.08	1.04	sema domain, transmembrane domain (TM), and cytoplasmic domain,

					(semaphorin) 6D
1372844_at	Efna1	2.16	2.31	-1.07	ephrin A1
1371545_at	Pecam1	2.16	2.31	-1.07	platelet/endothelial cell adhesion molecule 1
1381410_a_at	Fgd5	2.16	2.43	-1.13	FYVE, RhoGEF and PH domain containing 5
1398273_at	Efna1	2.15	2.43	-1.13	ephrin A1
1372084_at	Ptp4a3	2.15	2.06	1.05	protein tyrosine phosphatase type IVA, member 3
1371079_at	Fcgr2b	2.15	2.03	1.06	Fc fragment of IgG, low affinity IIb, receptor (CD32)
1379088_x_at	---	2.15	2.50	-1.17	---
1377046_at	Ankrd6	2.13	2.38	-1.12	ankyrin repeat domain 6
1379790_at	Dll4	2.13	2.32	-1.09	delta-like 4 (Drosophila)
1373661_a_at	Cxcr4	2.12	1.99	1.07	chemokine (C-X-C motif) receptor 4
1370302_at	Shroom2	2.12	2.07	1.02	shroom family member 2
1398256_at	Il1b	2.11	2.33	-1.10	interleukin 1 beta
1378486_at	---	2.11	1.92	1.09	---
1370948_a_at	Marcks	2.11	2.08	1.01	myristoylated alanine rich protein kinase C substrate
1375216_at	Pvrl2	2.10	2.33	-1.11	poliovirus receptor-related 2
1376876_at	---	2.10	2.19	-1.04	---
1389244_x_at	Cxcr4	2.09	1.93	1.09	chemokine (C-X-C motif) receptor 4
1375034_at	Pla2g15	2.09	2.17	-1.04	phospholipase A2, group XV
1369579_at	Stc2	2.08	1.80	1.16	stanniocalcin 2
1379381_at	Ciita	2.08	2.36	-1.13	class II, major histocompatibility complex, transactivator
1375523_at	Marcks	2.08	1.96	1.06	myristoylated alanine rich protein kinase C substrate
1398397_at	---	2.08	2.25	-1.08	---
1394367_at	Dll4	2.08	2.13	-1.02	delta-like 4 (Drosophila)
1398120_at	---	2.08	2.51	-1.21	---
1390965_at	---	2.07	2.26	-1.09	---
1370113_at	Birc3	2.06	2.24	-1.09	baculoviral IAP repeat-containing 3
1384484_at	LOC100359654	2.06	2.11	-1.02	synovial sarcoma, X breakpoint 2 interacting protein-like
1368300_at	Adora2a	2.06	2.09	-1.02	adenosine A2a receptor

1391260_at	---	2.05	2.16	-1.05	---
1371394_x_at	---	2.05	1.55	1.32	---
1377404_at	Stc1	2.05	1.77	1.16	stanniocalcin 1
1382404_at	---	2.05	2.33	-1.14	---
1369895_s_at	Podxl	2.05	2.13	-1.04	podocalyxin-like
1380338_at	---	2.04	1.94	1.05	---
1392220_at	Erg	2.04	2.31	-1.13	v-ets erythroblastosis virus E26 oncogene homolog (avian)
1370051_at	Tgm1	2.04	2.13	-1.04	transglutaminase 1
1385851_at	Capn5	2.03	2.20	-1.08	calpain 5
1391442_at	---	2.02	2.11	-1.05	---
1370483_at	Cd244	2.02	2.09	-1.04	Cd244 molecule, natural killer cell receptor 2B4
1387190_at	Dgka	2.01	2.15	-1.07	diacylglycerol kinase, alpha
1368882_at	St6galnac3	2.01	2.28	-1.14	ST6 (alpha-N-acetyl-neuraminyl-2,3-beta-galactosyl-1,3)-N-acetylgalactosaminide alpha-2
1382185_at	C1qtnf2	-2.02	-1.91	-1.06	C1q and tumor necrosis factor related protein 2
1396167_at	Acp6	-2.12	-1.82	-1.16	acid phosphatase 6, lysophosphatidic
1378233_at	---	-2.14	-2.11	-1.01	---
1372613_at	Bdh2	-2.14	-2.45	1.15	3-hydroxybutyrate dehydrogenase, type 2
1371003_at	Map1b	-2.17	-2.78	1.28	microtubule-associated protein 1B
1372626_at	Tpd52l1	-2.20	-2.14	-1.03	tumor protein D52-like 1
1398406_at	---	-2.21	-2.33	1.06	---
1390429_at	---	-2.24	-1.88	-1.19	---
1392963_at	Scrn1	-2.41	-2.52	1.05	secernin 1
1379932_at	Clcn4	-2.50	-2.42	-1.03	chloride channel, voltage-sensitive 4
1370291_at	Pdlim3	-2.74	-2.68	-1.02	PDZ and LIM domain 3
1387968_at	Slc6a15	-3.34	-3.59	1.07	solute carrier family 6 (neutral amino acid transporter), member 15
1393338_at	Scx	-3.66	-2.78	-1.32	scleraxis
1390596_at	Mlana	-3.89	-3.50	-1.11	melan-A

Table S2. Identified Canonical Pathways and Their Significantly Regulated Genes in Open Vs. Closed Comparison

Ingenuity Canonical Pathways	-log(p-value)	Ratio	Molecules
Antigen Presentation Pathway	5.30E-00	1.35E-01	CD74,HLA-DQA1,HLA-DRB5,HLA-DRA,CIITA
Graft-versus-Host Disease Signaling	4.73E-00	1.04E-01	IL1B,HLA-DQA1,HLA-DQB1,HLA-DRB5,HLA-DRA
Dendritic Cell Maturation	4.53E-00	4.52E-02	IRF8,FCGR2B,IL1B,HLA-DQA1,HLA-DQB1,HLA-DRB5,PIK3C2B,HLA-DRA
Altered T Cell and B Cell Signaling in Rheumatoid Arthritis	4.51E-00	6.82E-02	IL1B,TLR1,HLA-DQA1,HLA-DQB1,HLA-DRB5,HLA-DRA
B Cell Development	4.14E-00	1.21E-01	HLA-DQA1,HLA-DQB1,HLA-DRB5,HLA-DRA
iCOS-iCOSL Signaling in T Helper Cells	4.01E-00	5.56E-02	HLA-DQA1,HLA-DQB1,HLA-DRB5,PIK3C2B,LAT,HLA-DRA
CD28 Signaling in T Helper Cells	3.80E-00	5.08E-02	HLA-DQA1,HLA-DQB1,HLA-DRB5,PIK3C2B,LAT,HLA-DRA
PKCθ Signaling in T Lymphocytes	3.80E-00	5.08E-02	HLA-DQA1,HLA-DQB1,HLA-DRB5,PIK3C2B,LAT,HLA-DRA
TREM1 Signaling	3.79E-00	6.67E-02	IL1RL1,FCGR2B,IL1B,TLR1,CIITA
IL-4 Signaling	3.79E-00	6.67E-02	HLA-DQA1,HLA-DQB1,HLA-DRB5,PIK3C2B,HLA-DRA
Role of NFAT in Regulation of the Immune	3.76E-00	4.09E-02	FCGR2B,HLA-DQA1,HLA-DQB1,HLA-

Response			DRB5,PIK3C2B,LAT,HLA-DRA
Autoimmune Thyroid Disease Signaling	3.53E-00	8.51E-02	HLA-DQA1,HLA-DQB1,HLA-DRB5,HLA-DRA
Nur77 Signaling in T Lymphocytes	3.21E-00	7.02E-02	HLA-DQA1,HLA-DQB1,HLA-DRB5,HLA-DRA
Axonal Guidance Signaling	3.09E-00	2.30E-02	SEMA3G,ARHGEF15,CXCR4,VEGFA,SEMA6D,SEMA6A,PIK3C2B,ADAMTS9,EFNA1,BDNF
Type I Diabetes Mellitus Signaling	3.02E-00	4.55E-02	IL1B,HLA-DQA1,HLA-DQB1,HLA-DRB5,HLA-DRA
Calcium-induced T Lymphocyte Apoptosis	3.02E-00	6.25E-02	HLA-DQA1,HLA-DQB1,HLA-DRB5,HLA-DRA
IL-10 Signaling	2.92E-00	5.88E-02	CCR5,IL1RL1,FCGR2B,IL1B
T Helper Cell Differentiation	2.85E-00	5.63E-02	HLA-DQA1,HLA-DQB1,HLA-DRB5,HLA-DRA
Hepatic Fibrosis / Hepatic Stellate Cell Activation	2.79E-00	3.28E-02	CCR5,IL1RL1,IL1B,KDR,VEGFA,IGFBP3
Notch Signaling	2.66E-00	7.89E-02	MFNG,NOTCH4,DLL4
Allograft Rejection Signaling	2.58E-00	4.76E-02	HLA-DQA1,HLA-DQB1,HLA-DRB5,HLA-DRA
Communication between Innate and Adaptive Immune Cells	2.49E-00	4.49E-02	IL1B,TLR1,HLA-DRB5,HLA-DRA
OX40 Signaling Pathway	2.49E-00	4.49E-02	HLA-DQA1,HLA-DQB1,HLA-DRB5,HLA-DRA
NAD Phosphorylation and Dephosphorylation	2.46E-00	1.54E-01	ACP6,ACP5
Amyotrophic Lateral Sclerosis Signaling	2.34E-00	4.08E-02	CAPN5,VEGFA,PIK3C2B,BIRC3
Ephrin Receptor Signaling	2.16E-00	2.87E-02	SH2D3C,ARHGEF15,CXCR4,VEGFA,EFNA1

Granulocyte Adhesion and Diapedesis	2.13E-00	2.82E-02	IL1RL1,CXCR4,IL1B,CLDN5,PECAM1
IL-6 Signaling	2.08E-00	3.45E-02	IL1RL1,IL1B,VEGFA,PIK3C2B
Agranulocyte Adhesion and Diapedesis	2.01E-00	2.65E-02	CXCR4,IL1B,CLDN5,Podxl,PECAM1
Renal Cell Carcinoma Signaling	1.90E-00	4.23E-02	VEGFA,PIK3C2B,SLC2A1
NAD Salvage Pathway II	1.87E-00	7.69E-02	ACP6,ACP5
Toll-like Receptor Signaling	1.85E-00	4.05E-02	IL1RL1,IL1B,TLR1
VEGF Family Ligand-Receptor Interactions	1.82E-00	3.95E-02	KDR,VEGFA,PIK3C2B
Reelin Signaling in Neurons	1.77E-00	3.80E-02	RELN,ARHGEF15,PIK3C2B
Role of Osteoblasts, Osteoclasts and Chondrocytes in Rheumatoid Arthritis	1.76E-00	2.28E-02	IL1RL1,IL1B,ACP5,PIK3C2B,BIRC3
Tyrosine Biosynthesis IV	1.69E-00	3.33E-01	PCBD1
Inhibition of Angiogenesis by TSP1	1.65E-00	5.88E-02	KDR,VEGFA
Crosstalk between Dendritic Cells and Natural Killer Cells	1.64E-00	3.37E-02	HLA-DRB5,PVRL2,HLA-DRA
VEGF Signaling	1.60E-00	3.26E-02	KDR,VEGFA,PIK3C2B
Retinoate Biosynthesis II	1.57E-00	2.50E-01	RBP7
Phenylalanine Degradation I (Aerobic)	1.57E-00	2.50E-01	PCBD1
Cdc42 Signaling	1.56E-00	2.40E-02	HLA-DQA1,HLA-DQB1,HLA-DRB5,HLA-DRA
Docosahexaenoic Acid (DHA) Signaling	1.54E-00	5.13E-02	IL1B,PIK3C2B

NF-κB Signaling	1.51E-00	2.31E-02	IL1B,KDR,TLR1,PIK3C2B
Nitric Oxide Signaling in the Cardiovascular System	1.51E-00	3.00E-02	KDR,VEGFA,PIK3C2B
G-Protein Coupled Receptor Signaling	1.50E-00	1.95E-02	ADORA2A,APLNR,P2RY13,PIK3C2B,RGS16
Fcγ3RIIB Signaling in B Lymphocytes	1.50E-00	4.88E-02	FCGR2B,PIK3C2B
HIF1α Signaling	1.48E-00	2.94E-02	VEGFA,PIK3C2B,SLC2A1
Role of Hypercytokinemia/hyperchemokinemia in the Pathogenesis of Influenza	1.44E-00	4.55E-02	CCR5,IL1B
IL-8 Signaling	1.43E-00	2.17E-02	ANGPT2,KDR,VEGFA,PIK3C2B
phagosome formation	1.41E-00	2.75E-02	FCGR2B,TLR1,PIK3C2B
Natural Killer Cell Signaling	1.40E-00	2.73E-02	CD244,PIK3C2B,LAT
Role of Tissue Factor in Cancer	1.40E-00	2.73E-02	IL1B,VEGFA,PIK3C2B
Ephrin A Signaling	1.37E-00	4.17E-02	PIK3C2B,EFNA1
Leukocyte Extravasation Signaling	1.33E-00	2.02E-02	CXCR4,CLDN5,PIK3C2B,PECAM1
Role of Macrophages, Fibroblasts and Endothelial Cells in Rheumatoid Arthritis	1.28E-00	1.69E-02	IL1RL1,IL1B,VEGFA,TLR1,PIK3C2B
Role of Pattern Recognition Receptors in Recognition of Bacteria and Viruses	1.26E-00	2.38E-02	IL1B,TLR1,PIK3C2B
Pathogenesis of Multiple Sclerosis	1.22E-00	1.11E-01	CCR5
Ketolysis	1.22E-00	1.11E-01	BDH2

Systemic Lupus Erythematosus Signaling	1.22E-00	1.86E-02	FCGR2B,IL1B,PIK3C2B,LAT
Induction of Apoptosis by HIV1	1.20E-00	3.33E-02	CXCR4,BIRC3
LPS/IL-1 Mediated Inhibition of RXR Function	1.20E-00	1.83E-02	IL1RL1,IL1B,NR5A2,CHST1
Ketogenesis	1.18E-00	1.00E-01	BDH2
Role of PI3K/AKT Signaling in the Pathogenesis of Influenza	1.15E-00	3.12E-02	CCR5,PIK3C2B
Huntington's Disease Signaling	1.14E-00	1.75E-02	CAPN5,PIK3C2B,BDNF,TGM2
Mineralocorticoid Biosynthesis	1.14E-00	9.09E-02	Hsd3b1
eNOS Signaling	1.13E-00	2.11E-02	KDR,VEGFA,PIK3C2B
Angiopoietin Signaling	1.13E-00	3.03E-02	ANGPT2,PIK3C2B
Neurotrophin/TRK Signaling	1.11E-00	2.99E-02	PIK3C2B,BDNF
Glucocorticoid Biosynthesis	1.10E-00	8.33E-02	Hsd3b1
Phospholipase C Signaling	1.10E-00	1.69E-02	ARHGEF15,FCGR2B,LAT,TGM2
Growth Hormone Signaling	1.09E-00	2.90E-02	PIK3C2B,IGFBP3
PEDF Signaling	1.07E-00	2.82E-02	PIK3C2B,BDNF
Chemokine Signaling	1.07E-00	2.82E-02	CCR5,CXCR4
NF-κB Activation by Viruses	1.05E-00	2.74E-02	CCR5,PIK3C2B
Leptin Signaling in Obesity	1.04E-00	2.70E-02	PIK3C2B,NPY

Androgen Biosynthesis	1.04E-00	7.14E-02	Hsd3b1
3-phosphoinositide Biosynthesis	1.03E-00	1.90E-02	ACP5,PIK3C2B,PPP1R13B
The Visual Cycle	1.01E-00	6.67E-02	RBP7
Vitamin-C Transport	1.01E-00	6.67E-02	SLC2A1
VDR/RXR Activation	1.00E-00	2.56E-02	IL1RL1,IGFBP3
Hepatic Cholestasis	1.00E-00	1.85E-02	IL1RL1,IL1B,NR5A2
Wnt/β-catenin Signaling	9.61E-01	1.78E-02	SOX18,SOX7,NR5A2
TR/RXR Activation	9.40E-01	2.35E-02	PIK3C2B,SLC2A1
Differential Regulation of Cytokine Production in Macrophages and T Helper Cells by IL-17A and IL-17F	9.35E-01	5.56E-02	IL1B
FAK Signaling	9.24E-01	2.30E-02	CAPN5,PIK3C2B
CTLA4 Signaling in Cytotoxic T Lymphocytes	9.16E-01	2.27E-02	PIK3C2B,LAT
RANK Signaling in Osteoclasts	9.16E-01	2.27E-02	PIK3C2B,BIRC3
Apoptosis Signaling	9.08E-01	2.25E-02	CAPN5,BIRC3
AMPK Signaling	9.07E-01	1.68E-02	PIK3C2B,SLC2A1,AK4
PPAR Signaling	8.69E-01	2.13E-02	IL1RL1,IL1B
mTOR Signaling	8.61E-01	1.60E-02	PRR5L,VEGFA,PIK3C2B

Pyrimidine Deoxyribonucleotides De Novo Biosynthesis I	8.54E-01	4.55E-02	AK4
RAR Activation	8.51E-01	1.58E-02	VEGFA,RBP7,IGFBP3
IGF-1 Signaling	8.47E-01	2.06E-02	PIK3C2B,IGFBP3
T Cell Receptor Signaling	8.47E-01	2.06E-02	PIK3C2B,LAT
p53 Signaling	8.40E-01	2.04E-02	PIK3C2B,PPP1R13B
Differential Regulation of Cytokine Production in Intestinal Epithelial Cells by IL-17A and IL-17F	8.36E-01	4.35E-02	IL1B
Superpathway of Inositol Phosphate Compounds	8.27E-01	1.54E-02	ACP5,PIK3C2B,PPP1R13B
Neuropathic Pain Signaling In Dorsal Horn Neurons	8.26E-01	2.00E-02	PIK3C2B,BDNF
Tumoricidal Function of Hepatic Natural Killer Cells	8.19E-01	4.17E-02	LYVE1
Pancreatic Adenocarcinoma Signaling	7.86E-01	1.89E-02	VEGFA,PIK3C2B
Fc Epsilon RI Signaling	7.74E-01	1.85E-02	PIK3C2B,LAT
Corticotropin Releasing Hormone Signaling	7.55E-01	1.80E-02	VEGFA,BDNF
TNFR2 Signaling	7.44E-01	3.45E-02	BIRC3
Pyrimidine Ribonucleotides Interconversion	7.44E-01	3.45E-02	AK4
Role of p14/p19ARF in Tumor Suppression	7.31E-01	3.33E-02	PIK3C2B

cAMP-mediated signaling	7.24E-01	1.37E-02	ADORA2A,APLNR,P2RY13
p38 MAPK Signaling	7.21E-01	1.71E-02	IL1RL1,IL1B
Pyrimidine Ribonucleotides De Novo Biosynthesis	7.18E-01	3.23E-02	AK4
HMGB1 Signaling	7.04E-01	1.67E-02	IL1B,PIK3C2B
Gαi Signaling	7.04E-01	1.67E-02	APLNR,P2RY13
phagosome maturation	7.04E-01	1.67E-02	HLA-DRB5,HLA-DRA
LXR/RXR Activation	6.98E-01	1.65E-02	IL1RL1,IL1B
MIF-mediated Glucocorticoid Regulation	6.94E-01	3.03E-02	CD74
Retinoate Biosynthesis I	6.94E-01	3.03E-02	RBP7
Retinol Biosynthesis	6.94E-01	3.03E-02	RBP7
Atherosclerosis Signaling	6.83E-01	1.61E-02	CXCR4,IL1B
IL-9 Signaling	6.82E-01	2.94E-02	PIK3C2B
TWEAK Signaling	6.82E-01	2.94E-02	BIRC3
FXR/RXR Activation	6.67E-01	1.57E-02	IL1B,NR5A2
Colorectal Cancer Metastasis Signaling	6.60E-01	1.27E-02	VEGFA,TLR1,PIK3C2B
Stearate Biosynthesis I (Animals)	6.60E-01	2.78E-02	BDH2
D-myo-inositol (1,4,5,6)-Tetrakisphosphate Biosynthesis	6.52E-01	1.54E-02	ACP5,PPP1R13B

D-myo-inositol (3,4,5,6)-tetrakisphosphate Biosynthesis	6.52E-01	1.54E-02	ACP5,PPP1R13B
Complement System	6.50E-01	2.70E-02	CFD
Ovarian Cancer Signaling	6.47E-01	1.53E-02	VEGFA,PIK3C2B
IL-12 Signaling and Production in Macrophages	6.33E-01	1.49E-02	IRF8,PIK3C2B
Human Embryonic Stem Cell Pluripotency	6.33E-01	1.49E-02	PIK3C2B,BDNF
Relaxin Signaling	6.28E-01	1.48E-02	VEGFA,PIK3C2B
Thyroid Cancer Signaling	6.20E-01	2.50E-02	BDNF
MIF Regulation of Innate Immunity	6.11E-01	2.44E-02	CD74
Aryl Hydrocarbon Receptor Signaling	6.06E-01	1.43E-02	IL1B,TGM2
Melanoma Signaling	6.02E-01	2.38E-02	PIK3C2B
Role of IL-17F in Allergic Inflammatory Airway Diseases	5.84E-01	2.27E-02	IL1B
Dermatan Sulfate Biosynthesis (Late Stages)	5.84E-01	2.27E-02	CHST1
Serotonin Receptor Signaling	5.84E-01	2.27E-02	PCBD1
D-myo-inositol-5-phosphate Metabolism	5.80E-01	1.37E-02	ACP5,PPP1R13B
Epithelial Adherens Junction Signaling	5.80E-01	1.37E-02	PVRL2,NOTCH4
3-phosphoinositide Degradation	5.76E-01	1.36E-02	ACP5,PPP1R13B
Gα±q Signaling	5.76E-01	1.36E-02	PIK3C2B,RGS16

Role of Oct4 in Mammalian Embryonic Stem Cell Pluripotency	5.68E-01	2.17E-02	NR5A2
MSP-RON Signaling Pathway	5.68E-01	2.17E-02	PIK3C2B
Chondroitin Sulfate Biosynthesis (Late Stages)	5.68E-01	2.17E-02	CHST1
nNOS Signaling in Neurons	5.60E-01	2.13E-02	CAPN5
CXCR4 Signaling	5.56E-01	1.32E-02	CXCR4,PIK3C2B
Primary Immunodeficiency Signaling	5.52E-01	2.08E-02	CIITA
Xenobiotic Metabolism Signaling	5.49E-01	1.11E-02	IL1B,PIK3C2B,CHST1
TNFR1 Signaling	5.44E-01	2.04E-02	BIRC3
Heparan Sulfate Biosynthesis (Late Stages)	5.37E-01	2.00E-02	CHST1
Amyloid Processing	5.30E-01	1.96E-02	CAPN5
Germ Cell-Sertoli Cell Junction Signaling	5.25E-01	1.25E-02	PVRL2,PIK3C2B
CNTF Signaling	5.23E-01	1.92E-02	PIK3C2B
Endometrial Cancer Signaling	5.23E-01	1.92E-02	PIK3C2B
UVB-Induced MAPK Signaling	5.16E-01	1.89E-02	PIK3C2B
IL-2 Signaling	5.16E-01	1.89E-02	PIK3C2B
Lymphotoxin α2 Receptor Signaling	5.09E-01	1.85E-02	PIK3C2B
Role of IL-17A in Arthritis	5.09E-01	1.85E-02	PIK3C2B

Chondroitin Sulfate Biosynthesis	5.09E-01	1.85E-02	CHST1
Thrombopoietin Signaling	5.03E-01	1.82E-02	PIK3C2B
Role of Cytokines in Mediating Communication between Immune Cells	5.03E-01	1.82E-02	IL1B
Tight Junction Signaling	5.00E-01	1.20E-02	PVRL2,CLDN5
EGF Signaling	4.96E-01	1.79E-02	PIK3C2B
Acute Phase Response Signaling	4.93E-01	1.18E-02	IL1B,RBP7
Glioma Invasiveness Signaling	4.90E-01	1.75E-02	PIK3C2B
ErbB2-ErbB3 Signaling	4.90E-01	1.75E-02	PIK3C2B
Heparan Sulfate Biosynthesis	4.90E-01	1.75E-02	CHST1
Dermatan Sulfate Biosynthesis	4.90E-01	1.75E-02	CHST1
Regulation of Cellular Mechanics by Calpain Protease	4.90E-01	1.75E-02	CAPN5
Myc Mediated Apoptosis Signaling	4.84E-01	1.72E-02	PIK3C2B
B Cell Receptor Signaling	4.77E-01	1.15E-02	FCGR2B,PIK3C2B
ErbB4 Signaling	4.72E-01	1.67E-02	PIK3C2B
Sertoli Cell-Sertoli Cell Junction Signaling	4.64E-01	1.12E-02	PVRL2,CLDN5
PPARγ/RXRα Activation	4.61E-01	1.12E-02	IL1RL1,IL1B
GM-CSF Signaling	4.60E-01	1.61E-02	PIK3C2B

Production of Nitric Oxide and Reactive Oxygen Species in Macrophages	4.58E-01	1.11E-02	IRF8,PIK3C2B
Antiproliferative Role of Somatostatin Receptor 2	4.55E-01	1.59E-02	PIK3C2B
Estrogen-Dependent Breast Cancer Signaling	4.55E-01	1.59E-02	PIK3C2B
Role of JAK1 and JAK3 in γ3c Cytokine Signaling	4.55E-01	1.59E-02	PIK3C2B
IL-17A Signaling in Airway Cells	4.49E-01	1.56E-02	PIK3C2B
Regulation of the Epithelial-Mesenchymal Transition Pathway	4.46E-01	1.09E-02	PIK3C2B,NOTCH4
CD40 Signaling	4.44E-01	1.54E-02	PIK3C2B
Non-Small Cell Lung Cancer Signaling	4.44E-01	1.54E-02	PIK3C2B
Hypoxia Signaling in the Cardiovascular System	4.44E-01	1.54E-02	VEGFA
Clathrin-mediated Endocytosis Signaling	4.43E-01	1.08E-02	VEGFA,PIK3C2B
ILK Signaling	4.40E-01	1.08E-02	VEGFA,PIK3C2B
IL-15 Signaling	4.39E-01	1.52E-02	PIK3C2B
Mitotic Roles of Polo-Like Kinase	4.39E-01	1.52E-02	PLK2
Erythropoietin Signaling	4.33E-01	1.49E-02	PIK3C2B
GDNF Family Ligand-Receptor Interactions	4.28E-01	1.47E-02	PIK3C2B
Macropinocytosis Signaling	4.28E-01	1.47E-02	PIK3C2B

Thrombin Signaling	4.25E-01	1.05E-02	ARHGEF15,PIK3C2B
Breast Cancer Regulation by Stathmin1	4.25E-01	1.05E-02	ARHGEF15,PIK3C2B
CCR5 Signaling in Macrophages	4.23E-01	1.45E-02	CCR5
IL-3 Signaling	4.14E-01	1.41E-02	PIK3C2B
Small Cell Lung Cancer Signaling	4.14E-01	1.41E-02	PIK3C2B
IL-17 Signaling	4.09E-01	1.39E-02	PIK3C2B
JAK/Stat Signaling	4.09E-01	1.39E-02	PIK3C2B
LPS-stimulated MAPK Signaling	4.04E-01	1.37E-02	PIK3C2B
Prolactin Signaling	4.04E-01	1.37E-02	PIK3C2B
Ephrin B Signaling	4.04E-01	1.37E-02	CXCR4
STAT3 Pathway	4.04E-01	1.37E-02	KDR
FLT3 Signaling in Hematopoietic Progenitor Cells	4.00E-01	1.35E-02	PIK3C2B
Integrin Signaling	3.98E-01	9.95E-03	CAPN5,PIK3C2B
HER-2 Signaling in Breast Cancer	3.91E-01	1.32E-02	PIK3C2B
PDGF Signaling	3.87E-01	1.30E-02	PIK3C2B
Dopamine Receptor Signaling	3.82E-01	1.28E-02	PCBD1
Acute Myeloid Leukemia Signaling	3.78E-01	1.27E-02	PIK3C2B
Regulation of IL-2 Expression in Activated	3.78E-01	1.27E-02	LAT

and Anergic T Lymphocytes			
Ceramide Signaling	3.74E-01	1.25E-02	PIK3C2B
Prostate Cancer Signaling	3.66E-01	1.22E-02	PIK3C2B
Melanocyte Development and Pigmentation Signaling	3.58E-01	1.19E-02	PIK3C2B
FGF Signaling	3.55E-01	1.18E-02	PIK3C2B
ErbB Signaling	3.51E-01	1.16E-02	PIK3C2B
Bladder Cancer Signaling	3.47E-01	1.15E-02	VEGFA
UVA-Induced MAPK Signaling	3.43E-01	1.14E-02	PIK3C2B
Molecular Mechanisms of Cancer	3.41E-01	8.22E-03	ARHGEF15,PIK3C2B,BIRC3
Virus Entry via Endocytic Pathways	3.40E-01	1.12E-02	PIK3C2B
PAK Signaling	3.40E-01	1.12E-02	PIK3C2B
Death Receptor Signaling	3.29E-01	1.09E-02	BIRC3
Chronic Myeloid Leukemia Signaling	3.26E-01	1.08E-02	PIK3C2B
Salvage Pathways of Pyrimidine Ribonucleotides	3.26E-01	1.08E-02	AK4
SAPK/JNK Signaling	3.23E-01	1.06E-02	PIK3C2B
Signaling by Rho Family GTPases	3.22E-01	8.55E-03	ARHGEF15,PIK3C2B
Glioma Signaling	3.20E-01	1.05E-02	PIK3C2B

Mouse Embryonic Stem Cell Pluripotency	3.20E-01	1.05E-02	PIK3C2B
CDK5 Signaling	3.07E-01	1.01E-02	BDNF
Telomerase Signaling	3.07E-01	1.01E-02	PIK3C2B
Antioxidant Action of Vitamin C	3.07E-01	1.01E-02	SLC2A1
Cholecystokinin/Gastrin-mediated Signaling	3.01E-01	9.90E-03	IL1B
Paxillin Signaling	3.01E-01	9.90E-03	PIK3C2B
Rac Signaling	2.92E-01	9.62E-03	PIK3C2B
HGF Signaling	2.89E-01	9.52E-03	PIK3C2B
NGF Signaling	2.84E-01	9.35E-03	PIK3C2B
fMLP Signaling in Neutrophils	2.81E-01	9.26E-03	PIK3C2B
Renin-Angiotensin Signaling	2.78E-01	9.17E-03	PIK3C2B
Sphingosine-1-phosphate Signaling	2.78E-01	9.17E-03	PIK3C2B
Gαs Signaling	2.78E-01	9.17E-03	ADORA2A
Role of NANOG in Mammalian Embryonic Stem Cell Pluripotency	2.73E-01	9.01E-03	PIK3C2B
14-3-3-mediated Signaling	2.58E-01	8.55E-03	PIK3C2B
CCR3 Signaling in Eosinophils	2.58E-01	8.55E-03	PIK3C2B
Type II Diabetes Mellitus Signaling	2.58E-01	8.55E-03	PIK3C2B

GÎ±12/13 Signaling	2.58E-01	8.55E-03	PIK3C2B
PTEN Signaling	2.55E-01	8.47E-03	KDR
p70S6K Signaling	2.53E-01	8.40E-03	PIK3C2B
P2Y Purigenic Receptor Signaling Pathway	2.53E-01	8.40E-03	PIK3C2B
Glucocorticoid Receptor Signaling	2.50E-01	7.27E-03	IL1B,PIK3C2B
Gustation Pathway	2.48E-01	8.26E-03	P2RY13
PI3K Signaling in B Lymphocytes	2.33E-01	7.81E-03	FCGR2B
Hereditary Breast Cancer Signaling	2.31E-01	7.75E-03	PIK3C2B
Insulin Receptor Signaling	2.20E-01	7.46E-03	PIK3C2B
Regulation of eIF4 and p70S6K Signaling	1.98E-01	6.85E-03	PIK3C2B
Glioblastoma Multiforme Signaling	1.98E-01	6.85E-03	PIK3C2B

Table S3. Identified Canonical Pathways and Their Significantly Regulated Genes in Open Vs. Cycling Comparison.

Ingenuity Canonical Pathways	-log(p-value)	Ratio	Molecules
Antigen Presentation Pathway	5.33E+00	1.35E-01	"CD74,HLA-DQA1,HLA-DRB5,HLA-DRA,CIITA"
CD28 Signaling in T Helper Cells	4.82E+00	5.93E-02	"HLA-DQA1,HLA-DQB1,MAPK12,HLA-DRB5,PIK3C2B,LAT,HLA-DRA"
Graft-versus-Host Disease Signaling	4.76E+00	1.04E-01	"IL1B,HLA-DQA1,HLA-DQB1,HLA-DRB5,HLA-DRA"
Altered T Cell and B Cell Signaling in Rheumatoid Arthritis	4.54E+00	6.82E-02	"IL1B,TLR1,HLA-DQA1,HLA-DQB1,HLA-DRB5,HLA-DRA"
OX40 Signaling Pathway	4.51E+00	6.74E-02	"HLA-DQA1,HLA-DQB1,MAPK12,HLA-DRB5,RT1-EC2,HLA-DRA"
B Cell Development	4.16E+00	1.21E-01	"HLA-DQA1,HLA-DQB1,HLA-DRB5,HLA-DRA"
iCOS-iCOSL Signaling in T Helper Cells	4.04E+00	5.56E-02	"HLA-DQA1,HLA-DQB1,HLA-DRB5,PIK3C2B,LAT,HLA-DRA"
Type I Diabetes Mellitus Signaling	4.00E+00	5.45E-02	"IL1B,HLA-DQA1,HLA-DQB1,MAPK12,HLA-DRB5,HLA-DRA"
PKCq¸ Signaling in T Lymphocytes	3.83E+00	5.08E-02	"HLA-DQA1,HLA-DQB1,HLA-DRB5,PIK3C2B,LAT,HLA-DRA"
IL-4 Signaling	3.82E+00	6.67E-02	"HLA-DQA1,HLA-DQB1,HLA-DRB5,PIK3C2B,HLA-DRA"
Role of NFAT in Regulation of the Immune Response	3.79E+00	4.09E-02	"GNAI1,HLA-DQA1,HLA-DQB1,HLA-DRB5,PIK3C2B,LAT,HLA-DRA"
Dendritic Cell Maturation	3.70E+00	3.95E-02	"IL1B,HLA-DQA1,HLA-DQB1,MAPK12,HLA-DRB5,PIK3C2B,HLA-DRA"
Allograft Rejection Signaling	3.59E+00	5.95E-02	"HLA-DQA1,HLA-DQB1,HLA-DRB5,RT1-EC2,HLA-DRA"
Autoimmune Thyroid Disease Signaling	3.55E+00	8.51E-02	"HLA-DQA1,HLA-DQB1,HLA-DRB5,HLA-DRA"
Nur77 Signaling in T Lymphocytes	3.23E+00	7.02E-02	"HLA-DQA1,HLA-DQB1,HLA-DRB5,HLA-DRA"
HIF1a± Signaling	3.20E+00	4.90E-02	"VEGFA,EGLN3,MAPK12,PIK3C2B,SLC2A1"
Axonal Guidance Signaling	3.14E+00	2.30E-02	"GNAI1,SEMA3G,ARHGEF15,VEGFA,SEMA6A, UNC5B,PIK3C2B, ADAMTS9,EFNA1,BDNF"

Calcium-induced T Lymphocyte Apoptosis	3.04E+00	6.25E-02	"HLA-DQA1,HLA-DQB1,HLA-DRB5,HLA-DRA"
Cdc42 Signaling	3.02E+00	3.59E-02	"HLA-DQA1,HLA-DQB1,MAPK12,HLA-DRB5,RT1-EC2,HLA-DRA"
T Helper Cell Differentiation	2.87E+00	5.63E-02	"HLA-DQA1,HLA-DQB1,HLA-DRB5,HLA-DRA"
Renal Cell Carcinoma Signaling	2.87E+00	5.63E-02	"VEGFA,EGLN3,PIK3C2B,SLC2A1"
IL-8 Signaling	2.81E+00	3.26E-02	"GNAI1,ANGPT2,VEGFA,MAPK12,PIK3C2B,CDH1"
Reelin Signaling in Neurons	2.70E+00	5.06E-02	"RELN,ARHGEF15,MAPK12,PIK3C2B"
Notch Signaling	2.67E+00	7.89E-02	"MFNG,NOTCH4,DLL4"
Communication between Innate and Adaptive Immune Cells	2.51E+00	4.49E-02	"IL1B,TLR1,HLA-DRB5,HLA-DRA"
Amyotrophic Lateral Sclerosis Signaling	2.36E+00	4.08E-02	"CAPN5,VEGFA,PIK3C2B,BIRC3"
Ephrin Receptor Signaling	2.19E+00	2.87E-02	"SH2D3C,GNAI1,ARHGEF15,VEGFA,EFNA1"
Role of Tissue Factor in Cancer	2.18E+00	3.64E-02	"IL1B,VEGFA,MAPK12,PIK3C2B"
Corticotropin Releasing Hormone Signaling	2.17E+00	3.60E-02	"GNAI1,VEGFA,MAPK12,BDNF"
IL-6 Signaling	2.10E+00	3.45E-02	"IL1B,VEGFA,MAPK12,PIK3C2B"
Agranulocyte Adhesion and Diapedesis	2.04E+00	2.65E-02	"GNAI1,IL1B,CLDN5,Podxl,PECAM1"
Role of Pattern Recognition Receptors in Recognition of Bacteria and Viruses	1.98E+00	3.17E-02	"IL1B,TLR1,MAPK12,PIK3C2B"
Leukocyte Extravasation Signaling	1.96E+00	2.53E-02	"GNAI1,MAPK12,CLDN5,PIK3C2B,PECAM1"
PEDF Signaling	1.91E+00	4.23E-02	"MAPK12,PIK3C2B,BDNF"
Toll-like Receptor Signaling	1.86E+00	4.05E-02	"IL1B,TLR1,MAPK12"
TREM1 Signaling	1.85E+00	4.00E-02	"IL1B,TLR1,CIITA"
"Role of Osteoblasts, Osteoclasts and Chondrocytes in Rheumatoid Arthritis"	1.79E+00	2.28E-02	"IL1B,ACP5,MAPK12,PIK3C2B,BIRC3"
Epithelial Adherens Junction Signaling	1.77E+00	2.74E-02	"PVRL2,MAGI1,CDH1,NOTCH4"
Tyrosine Biosynthesis IV	1.70E+00	3.33E-01	PCBD1
Signaling by Rho Family GTPases	1.67E+00	2.14E-02	"GNAI1,ARHGEF15,MAPK12,PIK3C2B,CDH1"
RANK Signaling in Osteoclasts	1.67E+00	3.41E-02	"MAPK12,PIK3C2B,BIRC3"
Colorectal Cancer Metastasis Signaling	1.66E+00	2.12E-02	"VEGFA,TLR1,MAPK12,PIK3C2B,CDH1"
Inhibition of Angiogenesis by TSP1	1.66E+00	5.88E-02	"VEGFA,MAPK12"
3-phosphoinositide Biosynthesis	1.65E+00	2.53E-02	"PALD1,ACP5,PIK3C2B,PPP1R13B"
Crosstalk between Dendritic Cells and Natural Killer Cells	1.65E+00	3.37E-02	"HLA-DRB5,PVRL2,HLA-DRA"
Germ Cell-Sertoli Cell Junction Signaling	1.64E+00	2.50E-02	"MAPK12,PVRL2,PIK3C2B,CDH1"
Retinoate Biosynthesis II	1.57E+00	2.50E-01	RBP7

Phenylalanine Degradation I (Aerobic)	1.57E+00	2.50E-01	PCBD1
Wnt/b-catenin Signaling	1.56E+00	2.37E-02	"SOX18,CDH1,SOX7,NR5A2"
Docosahexaenoic Acid (DHA) Signaling	1.55E+00	5.13E-02	"IL1B,PIK3C2B"
G-Protein Coupled Receptor Signaling	1.53E+00	1.95E-02	"GNAI1,ADORA2A,APLNR,PIK3C2B,RGS16"
Thyroid Cancer Signaling	1.53E+00	5.00E-02	"CDH1,BDNF"
MIF Regulation of Innate Immunity	1.51E+00	4.88E-02	"CD74,MAPK12"
Fcg_RIIB Signaling in B Lymphocytes	1.51E+00	4.88E-02	"MAPK12,PIK3C2B"
Granulocyte Adhesion and Diapedesis	1.50E+00	2.26E-02	"GNAI1,IL1B,CLDN5,PECAM1"
Sertoli Cell-Sertoli Cell Junction Signaling	1.49E+00	2.25E-02	"MAPK12,PVRL2,CLDN5,CDH1"
Melanoma Signaling	1.49E+00	4.76E-02	"PIK3C2B,CDH1"
AMPK Signaling	1.48E+00	2.23E-02	"MAPK12,PIK3C2B,SLC2A1,AK4"
Pancreatic Adenocarcinoma Signaling	1.46E+00	2.83E-02	"VEGFA,MAPK12,PIK3C2B"
Fc Epsilon RI Signaling	1.44E+00	2.78E-02	"MAPK12,PIK3C2B,LAT"
ILK Signaling	1.43E+00	2.15E-02	"VEGFA,MAPK12,PIK3C2B,CDH1"
Molecular Mechanisms of Cancer	1.43E+00	1.64E-02	"GNAI1,ARHGEF15,MAPK12,PIK3C2B,CDH1,BIRC3"
Natural Killer Cell Signaling	1.42E+00	2.73E-02	"CD244,PIK3C2B,LAT"
Thrombin Signaling	1.39E+00	2.09E-02	"GNAI1,ARHGEF15,MAPK12,PIK3C2B"
Ephrin A Signaling	1.38E+00	4.17E-02	"PIK3C2B,EFNA1"
Superpathway of Inositol Phosphate Compounds	1.37E+00	2.05E-02	"PALD1,ACP5,PIK3C2B,PPP1R13B"
CCR3 Signaling in Eosinophils	1.35E+00	2.56E-02	"GNAI1,MAPK12,PIK3C2B"
Ga12/13 Signaling	1.35E+00	2.56E-02	"MAPK12,PIK3C2B,CDH1"
Amyloid Processing	1.33E+00	3.92E-02	"CAPN5,MAPK12"
HMGB1 Signaling	1.32E+00	2.50E-02	"IL1B,MAPK12,PIK3C2B"
Endometrial Cancer Signaling	1.32E+00	3.85E-02	"PIK3C2B,CDH1"
UVB-Induced MAPK Signaling	1.30E+00	3.77E-02	"MAPK12,PIK3C2B"
Role of IL-17A in Arthritis	1.29E+00	3.70E-02	"MAPK12,PIK3C2B"
FXR/RXR Activation	1.26E+00	2.36E-02	"IL1B,MAPK12,NR5A2"
EGF Signaling	1.26E+00	3.57E-02	"MAPK12,PIK3C2B"
"D-myo-inositol (1,4,5,6)-Tetrakisphosphate Biosynthesis"	1.24E+00	2.31E-02	"PALD1,ACP5,PPP1R13B"
"D-myo-inositol (3,4,5,6)-tetrakisphosphate Biosynthesis"	1.24E+00	2.31E-02	"PALD1,ACP5,PPP1R13B"
Myc Mediated Apoptosis Signaling	1.24E+00	3.45E-02	"MAPK12,PIK3C2B"
Ketolysis	1.23E+00	1.11E-01	BDH2

Induction of Apoptosis by HIV1	1.21E+00	3.33E-02	"MAPK12,BIRC3"
Relaxin Signaling	1.20E+00	2.22E-02	"GNAI1,VEGFA,PIK3C2B"
Ketogenesis	1.19E+00	1.00E-01	BDH2
Role of PI3K/AKT Signaling in the Pathogenesis of Influenza	1.16E+00	3.12E-02	"GNAI1,PIK3C2B"
IL-17A Signaling in Airway Cells	1.16E+00	3.12E-02	"MAPK12,PIK3C2B"
Huntington's Disease Signaling	1.16E+00	1.75E-02	"CAPN5,PIK3C2B,BDNF,TGM2"
CD40 Signaling	1.15E+00	3.08E-02	"MAPK12,PIK3C2B"
Mineralocorticoid Biosynthesis	1.15E+00	9.09E-02	Hsd3b1
IL-15 Signaling	1.14E+00	3.03E-02	"MAPK12,PIK3C2B"
Angiopoietin Signaling	1.14E+00	3.03E-02	"ANGPT2,PIK3C2B"
Neurotrophin/TRK Signaling	1.13E+00	2.99E-02	"PIK3C2B,BDNF"
D-myo-inositol-5-phosphate Metabolism	1.12E+00	2.05E-02	"PALD1,ACP5,PPP1R13B"
IL-10 Signaling	1.11E+00	2.94E-02	"IL1B,MAPK12"
GDNF Family Ligand-Receptor Interactions	1.11E+00	2.94E-02	"MAPK12,PIK3C2B"
3-phosphoinositide Degradation	1.11E+00	2.04E-02	"PALD1,ACP5,PPP1R13B"
Glucocorticoid Biosynthesis	1.11E+00	8.33E-02	Hsd3b1
CCR5 Signaling in Macrophages	1.10E+00	2.90E-02	"GNAI1,MAPK12"
Chemokine Signaling	1.08E+00	2.82E-02	"GNAI1,MAPK12"
CXCR4 Signaling	1.08E+00	1.97E-02	"GNAI1,MAPK12,PIK3C2B"
NAD Phosphorylation and Dephosphorylation	1.08E+00	7.69E-02	ACP5
IL-17 Signaling	1.07E+00	2.78E-02	"MAPK12,PIK3C2B"
LPS-stimulated MAPK Signaling	1.06E+00	2.74E-02	"MAPK12,PIK3C2B"
FLT3 Signaling in Hematopoietic Progenitor Cells	1.05E+00	2.70E-02	"MAPK12,PIK3C2B"
Leptin Signaling in Obesity	1.05E+00	2.70E-02	"PIK3C2B,NPY"
Tec Kinase Signaling	1.05E+00	1.91E-02	"GNAI1,MAPK12,PIK3C2B"
Androgen Biosynthesis	1.04E+00	7.14E-02	Hsd3b1
VEGF Family Ligand-Receptor Interactions	1.03E+00	2.63E-02	"VEGFA,PIK3C2B"
Hepatic Cholestasis	1.02E+00	1.85E-02	"IL1B,MAPK12,NR5A2"
The Visual Cycle	1.02E+00	6.67E-02	RBP7
Vitamin-C Transport	1.02E+00	6.67E-02	SLC2A1
Regulation of IL-2 Expression in Activated and Anergic T Lymphocytes	1.00E+00	2.53E-02	"MAPK12,LAT"
Parkinson's Signaling	9.89E-01	6.25E-02	MAPK12

Acute Phase Response Signaling	9.75E-01	1.78E-02	"IL1B,RBP7,MAPK12"
Endothelin-1 Signaling	9.58E-01	1.74E-02	"GNAI1,MAPK12,PIK3C2B"
Xenobiotic Metabolism Signaling	9.56E-01	1.48E-02	"IL1B,MAPK12,PIK3C2B,CHST1"
RhoGDI Signaling	9.53E-01	1.73E-02	"GNAI1,ARHGEF15,CDH1"
NF-kB Signaling	9.53E-01	1.73E-02	"IL1B,TLR1,PIK3C2B"
TR/RXR Activation	9.51E-01	2.35E-02	"PIK3C2B,SLC2A1"
FGF Signaling	9.51E-01	2.35E-02	"MAPK12,PIK3C2B"
ErbB Signaling	9.42E-01	2.33E-02	"MAPK12,PIK3C2B"
Differential Regulation of Cytokine Production in Macrophages and T Helper Cells by IL-17A and IL-17F	9.41E-01	5.56E-02	IL1B
Bladder Cancer Signaling	9.34E-01	2.30E-02	"VEGFA,CDH1"
FAK Signaling	9.34E-01	2.30E-02	"CAPN5,PIK3C2B"
CTLA4 Signaling in Cytotoxic T Lymphocytes	9.26E-01	2.27E-02	"PIK3C2B,LAT"
UVA-Induced MAPK Signaling	9.26E-01	2.27E-02	"MAPK12,PIK3C2B"
Role of NFAT in Cardiac Hypertrophy	9.20E-01	1.68E-02	"GNAI1,MAPK12,PIK3C2B"
PAK Signaling	9.18E-01	2.25E-02	"MAPK12,PIK3C2B"
Apoptosis Signaling	9.18E-01	2.25E-02	"CAPN5,BIRC3"
IL-1 Signaling	9.02E-01	2.20E-02	"GNAI1,MAPK12"
VEGF Signaling	8.94E-01	2.17E-02	"VEGFA,PIK3C2B"
Regulation of the Epithelial-Mesenchymal Transition Pathway	8.94E-01	1.63E-02	"PIK3C2B,CDH1,NOTCH4"
SAPK/JNK Signaling	8.79E-01	2.13E-02	"MAPK12,PIK3C2B"
mTOR Signaling	8.74E-01	1.60E-02	"PRR5L,VEGFA,PIK3C2B"
Mouse Embryonic Stem Cell Pluripotency	8.72E-01	2.11E-02	"MAPK12,PIK3C2B"
RAR Activation	8.64E-01	1.58E-02	"VEGFA,RBP7,MAPK12"
Pyrimidine Deoxyribonucleotides De Novo Biosynthesis I	8.60E-01	4.55E-02	AK4
Breast Cancer Regulation by Stathmin1	8.59E-01	1.57E-02	"GNAI1,ARHGEF15,PIK3C2B"
T Cell Receptor Signaling	8.57E-01	2.06E-02	"PIK3C2B,LAT"
"Role of Macrophages, Fibroblasts and Endothelial Cells in Rheumatoid Arthritis"	8.55E-01	1.35E-02	"IL1B,VEGFA,TLR1,PIK3C2B"
p53 Signaling	8.50E-01	2.04E-02	"PIK3C2B,PPP1R13B"
CDK5 Signaling	8.43E-01	2.02E-02	"MAPK12,BDNF"
Antioxidant Action of Vitamin C	8.43E-01	2.02E-02	"MAPK12,SLC2A1"

Differential Regulation of Cytokine Production in Intestinal Epithelial Cells by IL-17A and IL-17F	8.42E-01	4.35E-02	IL1B
Neuropathic Pain Signaling In Dorsal Horn Neurons	8.36E-01	2.00E-02	"PIK3C2B,BDNF"
Nitric Oxide Signaling in the Cardiovascular System	8.36E-01	2.00E-02	"VEGFA,PIK3C2B"
Cholecystokinin/Gastrin-mediated Signaling	8.29E-01	1.98E-02	"IL1B,MAPK12"
Paxillin Signaling	8.29E-01	1.98E-02	"MAPK12,PIK3C2B"
IL-22 Signaling	8.25E-01	4.17E-02	MAPK12
Tumoricidal Function of Hepatic Natural Killer Cells	8.25E-01	4.17E-02	LYVE1
IL-17A Signaling in Gastric Cells	8.08E-01	4.00E-02	MAPK12
Role of JAK family kinases in IL-6-type Cytokine Signaling	8.08E-01	4.00E-02	MAPK12
HGF Signaling	8.03E-01	1.90E-02	"MAPK12,PIK3C2B"
NAD Salvage Pathway II	7.93E-01	3.85E-02	ACP5
NGF Signaling	7.90E-01	1.87E-02	"MAPK12,PIK3C2B"
fMLP Signaling in Neutrophils	7.84E-01	1.85E-02	"GNAI1,PIK3C2B"
Renin-Angiotensin Signaling	7.77E-01	1.83E-02	"MAPK12,PIK3C2B"
Sphingosine-1-phosphate Signaling	7.77E-01	1.83E-02	"GNAI1,PIK3C2B"
phagosome formation	7.77E-01	1.83E-02	"TLR1,PIK3C2B"
Systemic Lupus Erythematosus Signaling	7.53E-01	1.40E-02	"IL1B,PIK3C2B,LAT"
TNFR2 Signaling	7.50E-01	3.45E-02	BIRC3
Pyrimidine Ribonucleotides Interconversion	7.50E-01	3.45E-02	AK4
LPS/IL-1 Mediated Inhibition of RXR Function	7.36E-01	1.37E-02	"IL1B,NR5A2,CHST1"
cAMP-mediated signaling	7.36E-01	1.37E-02	"GNAI1,ADORA2A,APLNR"
Role of p14/p19ARF in Tumor Suppression	7.36E-01	3.33E-02	PIK3C2B
14-3-3-mediated Signaling	7.30E-01	1.71E-02	"MAPK12,PIK3C2B"
Type II Diabetes Mellitus Signaling	7.30E-01	1.71E-02	"MAPK12,PIK3C2B"
p38 MAPK Signaling	7.30E-01	1.71E-02	"IL1B,MAPK12"
4-1BB Signaling in T Lymphocytes	7.24E-01	3.23E-02	MAPK12
Pyrimidine Ribonucleotides De Novo Biosynthesis	7.24E-01	3.23E-02	AK4
Cardiac Hypertrophy Signaling	7.21E-01	1.35E-02	"GNAI1,MAPK12,PIK3C2B"

p70S6K Signaling	7.19E-01	1.68E-02	"GNAI1,PIK3C2B"
P2Y Purigenic Receptor Signaling Pathway	7.19E-01	1.68E-02	"GNAI1,PIK3C2B"
Gai Signaling	7.13E-01	1.67E-02	"GNAI1,APLNR"
phagosome maturation	7.13E-01	1.67E-02	"HLA-DRB5,HLA-DRA"
MIF-mediated Glucocorticoid Regulation	6.99E-01	3.03E-02	CD74
Retinoate Biosynthesis I	6.99E-01	3.03E-02	RBP7
Retinol Biosynthesis	6.99E-01	3.03E-02	RBP7
IL-9 Signaling	6.88E-01	2.94E-02	PIK3C2B
TWEAK Signaling	6.88E-01	2.94E-02	BIRC3
IL-17A Signaling in Fibroblasts	6.76E-01	2.86E-02	MAPK12
Phospholipase C Signaling	6.69E-01	1.27E-02	"ARHGEF15,LAT,TGM2"
GNRH Signaling	6.66E-01	1.55E-02	"GNAI1,MAPK12"
Stearate Biosynthesis I (Animals)	6.66E-01	2.78E-02	BDH2
Ovarian Cancer Signaling	6.57E-01	1.53E-02	"VEGFA,PIK3C2B"
Complement System	6.55E-01	2.70E-02	CFD
April Mediated Signaling	6.45E-01	2.63E-02	MAPK12
IL-12 Signaling and Production in Macrophages	6.42E-01	1.49E-02	"MAPK12,PIK3C2B"
Human Embryonic Stem Cell Pluripotency	6.42E-01	1.49E-02	"PIK3C2B,BDNF"
Netrin Signaling	6.35E-01	2.56E-02	UNC5B
B Cell Activating Factor Signaling	6.25E-01	2.50E-02	MAPK12
Aryl Hydrocarbon Receptor Signaling	6.15E-01	1.43E-02	"IL1B,TGM2"
UVC-Induced MAPK Signaling	6.07E-01	2.38E-02	MAPK12
eNOS Signaling	6.06E-01	1.41E-02	"VEGFA,PIK3C2B"
Role of Hypercytokinemia/hyperchemokinemia in the Pathogenesis of Influenza	5.90E-01	2.27E-02	IL1B
Role of IL-17F in Allergic Inflammatory Airway Diseases	5.90E-01	2.27E-02	IL1B
iNOS Signaling	5.90E-01	2.27E-02	MAPK12
Dermatan Sulfate Biosynthesis (Late Stages)	5.90E-01	2.27E-02	CHST1
Serotonin Receptor Signaling	5.90E-01	2.27E-02	PCBD1
Regulation of eIF4 and p70S6K Signaling	5.89E-01	1.37E-02	"MAPK12,PIK3C2B"
Gaq Signaling	5.85E-01	1.36E-02	"PIK3C2B,RGS16"
Role of Oct4 in Mammalian Embryonic	5.73E-01	2.17E-02	NR5A2

Stem Cell Pluripotency			
MSP-RON Signaling Pathway	5.73E-01	2.17E-02	PIK3C2B
Chondroitin Sulfate Biosynthesis (Late Stages)	5.73E-01	2.17E-02	CHST1
nNOS Signaling in Neurons	5.65E-01	2.13E-02	CAPN5
Primary Immunodeficiency Signaling	5.57E-01	2.08E-02	CIITA
Gap Junction Signaling	5.53E-01	1.29E-02	"GNAI1,PIK3C2B"
TNFR1 Signaling	5.50E-01	2.04E-02	BIRC3
Glucocorticoid Receptor Signaling	5.49E-01	1.09E-02	"IL1B,MAPK12,PIK3C2B"
Heparan Sulfate Biosynthesis (Late Stages)	5.42E-01	2.00E-02	CHST1
CD27 Signaling in Lymphocytes	5.28E-01	1.92E-02	MAPK12
CNTF Signaling	5.28E-01	1.92E-02	PIK3C2B
IL-2 Signaling	5.21E-01	1.89E-02	PIK3C2B
Lymphotoxina_ Receptor Signaling	5.14E-01	1.85E-02	PIK3C2B
Chondroitin Sulfate Biosynthesis	5.14E-01	1.85E-02	CHST1
Tight Junction Signaling	5.09E-01	1.20E-02	"PVRL2,CLDN5"
Thrombopoietin Signaling	5.08E-01	1.82E-02	PIK3C2B
Role of Cytokines in Mediating Communication between Immune Cells	5.08E-01	1.82E-02	IL1B
Glioma Invasiveness Signaling	4.95E-01	1.75E-02	PIK3C2B
ErbB2-ErbB3 Signaling	4.95E-01	1.75E-02	PIK3C2B
Heparan Sulfate Biosynthesis	4.95E-01	1.75E-02	CHST1
Dermatan Sulfate Biosynthesis	4.95E-01	1.75E-02	CHST1
Regulation of Cellular Mechanics by Calpain Protease	4.95E-01	1.75E-02	CAPN5
CREB Signaling in Neurons	4.95E-01	1.17E-02	"GNAI1,PIK3C2B"
B Cell Receptor Signaling	4.85E-01	1.15E-02	"MAPK12,PIK3C2B"
ATM Signaling	4.83E-01	1.69E-02	MAPK12
ErbB4 Signaling	4.77E-01	1.67E-02	PIK3C2B
Production of Nitric Oxide and Reactive Oxygen Species in Macrophages	4.66E-01	1.11E-02	"MAPK12,PIK3C2B"
GM-CSF Signaling	4.65E-01	1.61E-02	PIK3C2B
Activation of IRF by Cytosolic Pattern Recognition Receptors	4.60E-01	1.59E-02	MAPK12
Antiproliferative Role of Somatostatin Receptor 2	4.60E-01	1.59E-02	PIK3C2B

Estrogen-Dependent Breast Cancer Signaling	4.60E-01	1.59E-02	PIK3C2B
Role of JAK1 and JAK3 in gc Cytokine Signaling	4.60E-01	1.59E-02	PIK3C2B
PCP pathway	4.60E-01	1.59E-02	MAPK12
Hepatic Fibrosis / Hepatic Stellate Cell Activation	4.57E-01	1.09E-02	"IL1B,VEGFA"
Clathrin-mediated Endocytosis Signaling	4.51E-01	1.08E-02	"VEGFA,PIK3C2B"
Non-Small Cell Lung Cancer Signaling	4.49E-01	1.54E-02	PIK3C2B
Hypoxia Signaling in the Cardiovascular System	4.49E-01	1.54E-02	VEGFA
Mitotic Roles of Polo-Like Kinase	4.44E-01	1.52E-02	PLK2
Erythropoietin Signaling	4.38E-01	1.49E-02	PIK3C2B
Remodeling of Epithelial Adherens Junctions	4.33E-01	1.47E-02	CDH1
Macropinocytosis Signaling	4.33E-01	1.47E-02	PIK3C2B
Agrin Interactions at Neuromuscular Junction	4.28E-01	1.45E-02	MAPK12
Growth Hormone Signaling	4.28E-01	1.45E-02	PIK3C2B
Role of MAPK Signaling in the Pathogenesis of Influenza	4.28E-01	1.45E-02	MAPK12
Melatonin Signaling	4.23E-01	1.43E-02	GNAI1
IL-3 Signaling	4.19E-01	1.41E-02	PIK3C2B
Small Cell Lung Cancer Signaling	4.19E-01	1.41E-02	PIK3C2B
GPCR-Mediated Integration of Enteroendocrine Signaling Exemplified by an L Cell	4.19E-01	1.41E-02	GNAI1
JAK/Stat Signaling	4.14E-01	1.39E-02	PIK3C2B
NF-kB Activation by Viruses	4.09E-01	1.37E-02	PIK3C2B
Prolactin Signaling	4.09E-01	1.37E-02	PIK3C2B
Ephrin B Signaling	4.09E-01	1.37E-02	GNAI1
STAT3 Pathway	4.09E-01	1.37E-02	MAPK12
Integrin Signaling	4.06E-01	9.95E-03	"CAPN5,PIK3C2B"
HER-2 Signaling in Breast Cancer	3.96E-01	1.32E-02	PIK3C2B
BMP signaling pathway	3.96E-01	1.32E-02	MAPK12
PDGF Signaling	3.91E-01	1.30E-02	PIK3C2B

Dopamine Receptor Signaling	3.87E-01	1.28E-02	PCBD1
Acute Myeloid Leukemia Signaling	3.83E-01	1.27E-02	PIK3C2B
Ceramide Signaling	3.79E-01	1.25E-02	PIK3C2B
Prostate Cancer Signaling	3.71E-01	1.22E-02	PIK3C2B
Melanocyte Development and Pigmentation Signaling	3.63E-01	1.19E-02	PIK3C2B
GPCR-Mediated Nutrient Sensing in Enteroendocrine Cells	3.63E-01	1.19E-02	GNAI1
a-Adrenergic Signaling	3.52E-01	1.15E-02	GNAI1
TGF-b Signaling	3.52E-01	1.15E-02	MAPK12
G Beta Gamma Signaling	3.48E-01	1.14E-02	GNAI1
Virus Entry via Endocytic Pathways	3.44E-01	1.12E-02	PIK3C2B
Death Receptor Signaling	3.34E-01	1.09E-02	BIRC3
Chronic Myeloid Leukemia Signaling	3.31E-01	1.08E-02	PIK3C2B
Salvage Pathways of Pyrimidine Ribonucleotides	3.31E-01	1.08E-02	AK4
PPAR Signaling	3.27E-01	1.06E-02	IL1B
Glioma Signaling	3.24E-01	1.05E-02	PIK3C2B
IGF-1 Signaling	3.18E-01	1.03E-02	PIK3C2B
Telomerase Signaling	3.11E-01	1.01E-02	PIK3C2B
Rac Signaling	2.96E-01	9.62E-03	PIK3C2B
Gas Signaling	2.82E-01	9.17E-03	ADORA2A
Androgen Signaling	2.77E-01	9.01E-03	GNAI1
Role of NANOG in Mammalian Embryonic Stem Cell Pluripotency	2.77E-01	9.01E-03	PIK3C2B
PTEN Signaling	2.59E-01	8.47E-03	MAGI1
LXR/RXR Activation	2.52E-01	8.26E-03	IL1B
Atherosclerosis Signaling	2.45E-01	8.06E-03	IL1B
Hereditary Breast Cancer Signaling	2.35E-01	7.75E-03	PIK3C2B
Insulin Receptor Signaling	2.24E-01	7.46E-03	PIK3C2B
Synaptic Long Term Depression	2.09E-01	7.04E-03	GNAI1
Glioblastoma Multiforme Signaling	2.02E-01	6.85E-03	PIK3C2B

Table S4. Target Genes and Their Fold-Changes for the Major Identified Regulators

Vegf target genes

Gene Name	Fold changes	Prediction
VEGFA	2.685	Activated
TBC1D8	2.563	Activated
STC1	2.435	Activated
NR5A2	2.073	Activated
NOTCH4	2.631	Activated
LYVE1	3.367	Activated
KDR	10.39	Activated
IGFBP3	4.025	Activated
EFNA1	2.158	Activated
DLL4	2.127	Activated
CXCR4	2.223	Activated
APLNR	10.691	Activated
APLN	3.48	Activated
ANGPT2	5.332	Activated
ADORA2A	2.058	Activated
RAMP3	2.714	Inhibited

Hif1α target genes

Gene Name	Fold changes	Prediction
VEGFA	2.685	Activated
SLC2A1	2.238	Activated
PDK1	2.243	Activated
NRARP	2.425	Activated
IL1B	2.11	Activated
IGFBP3	4.025	Activated
ERO1A	2.608	Activated
CXCR4	2.223	Activated
CA9	5.969	Activated
CCR5	2.52	Inhibited
ANKRD37	2.243	Affected

APLN	3.48	Affected
DLL4	2.127	Affected
SLC40A1	2.533	Affected
STC2	2.084	Affected

TNF target genes

Gene Name	Fold changes	Prediction
VEGFA	2.685	Activated
TGM2	3.287	Activated
SLC2A1	2.238	Activated
RGS16	3.413	Activated
NR5A2	2.073	Activated
NOTCH4	2.631	Activated
MMD	3.566	Activated
LRG1	2.657	Activated
KDR	10.39	Activated
IRF8	2.453	Activated
IL1RL1	3.533	Activated
IL1B	2.11	Activated
IGFBP3	4.025	Activated
HLA-DRA	16.17	Activated
FCGR2B	2.149	Activated
EFNA1	2.158	Activated
EBI3	2.572	Activated
CXCR4	2.223	Activated
C10orf10	3.321	Activated
BIRC3	2.061	Activated
BDNF	2.419	Activated
APLN	3.48	Activated
ANGPT2	5.332	Activated
ADORA2A	2.058	Activated
LYVE1	3.367	Inhibited
LAMA4	2.372	Inhibited
ERG	2.039	Inhibited
CIITA	2.083	Inhibited
CFD	4.258	Inhibited
CCR5	2.52	Inhibited
ACP5	5.037	Affected
PECAM1	2.158	Affected
PLK2	2.667	Affected

PRDM1	3.173	Affected

VIDEO S1

Video recording of the aortic valve grafts mounted in the bioreactor under flow conditions.

The grafts are imaged from the ventricular side of the outflow tract to demonstrate valve cycling with coaptation. The first 4 valves are in the Cycling condition. The next 4 valves are in the Closed position with sustained coaptation. The video ends with a return to the first Cycling valve shown at the start of the sequence.